

# The phase diagram of quantum gravity from diffeomorphism-invariant RG-flows

Ivan Donkin<sup>1</sup> and Jan M. Pawłowski<sup>1,2</sup>

<sup>1</sup>*Institut für Theoretische Physik, Universität Heidelberg,  
Philosophenweg 16, D-69120 Heidelberg, Germany*

<sup>2</sup>*ExtreMe Matter Institute EMMI, GSI Helmholtzzentrum für  
Schwerionenforschung mbH, Planckstr. 1, D-64291 Darmstadt, Germany*

We evaluate the phase diagram of quantum gravity within a fully diffeomorphism-invariant renormalisation group approach. The construction is based on the geometrical or Vilkovisky-DeWitt effective action. We also resolve the difference between the fluctuation metric and the background metric. This allows for fully background-independent flows in gravity.

The results provide further evidence for the ultraviolet fixed point scenario in quantum gravity with quantitative changes for the fixed point physics. We also find a stable infrared fixed point related to classical Einstein gravity. Implications and possible extensions are discussed.

PACS numbers: 05.10.Cc, 12.38.Aw, 11.10.Wx

## I. INTRODUCTION

In the past decade the asymptotic safety scenario of quantum gravity [1] has been explored in quite some detail. Evidence for a non-trivial UV fixed point (FP) has been collected with various methods, see e.g. [2–8]. Renormalisation group (RG) approaches to quantum gravity are naturally well-suited to study such a scenario. In its modern functional form the renormalisation group is by now very-well developed with many results in various physics areas, for reviews on gravity and gauge theories see e.g. [6–12]. Since the early works on the functional RG (FRG) [13–15], which were carried out within the Einstein-Hilbert approximation, our understanding of the underlying physics has been extended tremendously, for reviews see e.g. [6–8, 12]. In particular, the stability of the fixed point scenario has been tested far beyond the original Einstein-Hilbert truncation. These extensions include effects generated by the Weyl tensor as well by general terms in the curvature scalar, e.g. [16, 17], higher order derivative terms, e.g. [18, 19], ghost fluctuations, e.g. [20–22], first attempts on Lorenzian gravity, e.g. [23], as well as the coupling to matter and gauge fields, e.g. [24–28].

The impressive plethora of results, including those obtained in other approaches, [2–5, 7, 8], give us a firm grip on the asymptotic safety scenario in quantum gravity. This allows us to study interesting physics related to cosmology and the dynamics of the full matter-gravity system. Still, all approaches to quantum gravity have to face the non-trivial task of implementing full diffeomorphism invariance and reparameterisation invariance of the theory. This task is tightly linked to the question of background independence of quantum gravity which is also not fully resolved yet.

In the present work diffeomorphism invariance and background independence are discussed within the functional RG approach to gravity. This approach is based on the standard background field approach to quantum field theory, in which the theory is expanded about a specific

background field configuration. In gravity this is usually realised within a linear splitting of the full metric  $g$  in a background metric  $\bar{g}$  and a fluctuation  $h = g - \bar{g}$ . Finally, the background is identified with the dynamical metric by setting  $h = 0$ , which removes the background field dependence, see e.g. [29]. In this approach the effective action is invariant under symmetry transformations of the background field configuration. At its root this is only an auxiliary symmetry whereas the dynamical symmetry transformations of the fluctuations are non-trivially realised. Note, however, that the fluctuation field  $h$  in such an approach has no geometrical meaning, i.e. in gravity  $h$  is no metric, and in the simpler example of a Yang-Mills theory the fluctuation field is no connection.

Moreover, the symmetry identities of the fluctuation fields lead to non-linear relations between fluctuation field Green functions. It is also possible to derive identities that link background field Green functions and fluctuation field Green functions, the Nielsen identities [30]. The Nielsen identity in combination with the gauge/diffeomorphism covariance of the background field Green functions provide the non-trivial symmetry identities of the fluctuation field. In summary these relations are chiefly important for the discussion of diffeomorphism invariance as well as background independence in quantum gravity, and are at the root of the interpretation of the background correlation functions as S-matrix elements.

In the present work we put forward a fully diffeomorphism-invariant FRG approach to quantum gravity, [9, 31–33], by using the geometrical or Vilkovisky-DeWitt effective action, e.g. [34–39]. Our construction can be understood as a non-linear upgrade of the standard background field approach, its linear order giving precisely the background field relations in the Landau-DeWitt gauge. The gain of such a non-linear approach is that the fluctuation fields have a geometrical meaning and can be utilised to compute an effective action which only depends on the diffeomorphism-invariant part of the fluctuation fields. Consequently, the geometrical effective action is trivially diffeomorphism-

invariant, and any cutoff procedure applied to these fluctuation fields maintains diffeomorphism invariance. Still, fluctuation field Green functions and background metric Green functions are related to each other by means of a regulator-dependent Nielsen identity [9, 32].

Within this framework, we provide the first fully diffeomorphism-invariant evaluation of the phase diagram of quantum gravity including the infrared sector of the theory. Our approach also allows for a more direct access to the question of background independence. In a first non-trivial approximation the present work provides further evidence for the asymptotic safety scenario of quantum gravity. We also unravel an interesting infrared fixed point structure.

In Section II we briefly recapitulate the geometrical approach to quantum gravity. Its FRG version as formulated in [31, 32] is introduced in Section III. In Section IV we define the approximation which captures the difference between background metric dependence and fluctuation metric dependence. In Section V the Nielsen identity for the regularised geometrical effective action, [9, 32], is used to derive relations between different terms in the effective action. In Section VI we compute the UV fixed point within the geometrical approach in the Einstein-Hilbert truncation without the Nielsen identity. In Section VII we utilise the Nielsen identity to derive both the flow of the background couplings as well as that of the dynamical couplings. Results on the UV fixed point scenario within the geometrical approach in the standard background approximation are presented in Section VIII. In four space-time dimensions they agree with that obtained in the standard background field approach within the same background approximation, and in Landau-DeWitt gauge. In Section IX we present the results for the phase diagram of quantum gravity within the fully dynamical approach. The UV-fixed point scenario agrees qualitatively with that found in the background field approximation, and compares well with that found in the bi-metric background field approach put forward in [40], see Section IX A. We also find a stable infrared fixed point, see Section IX B, and show that the theory tends towards classical Einstein gravity in the infrared, see Section IX C. We close with a brief summary and discussion in Section X.

## II. GEOMETRICAL EFFECTIVE ACTION

In this Section we briefly review the geometrical approach to quantum field theory using the notation from [9, 32, 33, 37]. The geometrical approach hinges on the observation that the standard path integral has no manifest reparameterisation invariance. Put differently, its standard formulation assumes a flat path integral measure  $d\varphi$  for a given field theory with field  $\varphi$ . Neither such a measure nor the related source term  $\int_x J\varphi$  is invariant under field reparameterisations. This apparent non-invariance can be cured by enhancing the flat mea-

sure by an appropriately defined determinant  $\sqrt{\det \gamma}$  of the metric in field space,  $\gamma$ , and using a reparameterisation invariant source term  $\int_x J\phi(\bar{\varphi}, \varphi)$ . Here,  $\phi$  is chosen to be a geodesic normal field, i.e. it is the Gaussian normal coordinate representation of the fluctuating field  $\varphi$  with respect to a chosen background  $\bar{\varphi}$ . In linear approximation,  $\phi = \varphi - \bar{\varphi}$ , this reduces to the standard background field approach.

In gravity the field  $\varphi$  is the metric  $g$  and the classical action is the Einstein-Hilbert action  $S$ ,

$$S[g] = 2\kappa^2 \int d^d x \sqrt{g} \left( -R(g) + 2\Lambda \right), \quad (1)$$

with curvature scalar  $R$  and cosmological constant  $\Lambda$ . The prefactor  $\kappa^2$  is given by

$$\kappa^2 = \frac{1}{32\pi G_N}. \quad (2)$$

where  $G_N$  is the Newton constant. The basic object in the geometrical approach to gravity is the configuration space of the theory,  $\Phi = \{g_{\mu\nu}\}$ , equipped with the natural action of the diffeomorphism group  $\mathcal{G}$ . There is a one-parameter family of ultralocal group-invariant supermetrics on  $\Phi$

$$\begin{aligned} \gamma^{\mu\nu\rho'\sigma'}(x, x') = & \left[ \frac{1}{2} g^{\mu\rho'}(x) g^{\nu\sigma'}(x) + \frac{1}{2} g^{\mu\sigma'}(x) g^{\nu\rho'}(x) \right. \\ & \left. - \theta g^{\mu\nu}(x) g^{\rho'\sigma'}(x) \right] \sqrt{g(x)} \sqrt{g(x')} \delta(x, x') \end{aligned} \quad (3)$$

labelled by a continuous real parameter  $\theta$ . For the remainder of the paper we fix  $\theta = -1$ .

In the standard background field approach one expands the metric  $g$  about a given background metric  $\bar{g}$  within a linear split,  $g = \bar{g} + h$  with fluctuation field  $h$ . Such a parameterisation entails that the fluctuation  $h$  is neither a metric nor a vector, i.e. it has no geometrical meaning. In turn, within the geometrical approach we define  $h$  as a tangent vector at  $\bar{g}$  and  $\sigma^a[\bar{g}; g] = -h^a$  as the geodesic normal coordinate of  $g$  with respect to  $\bar{g}$ , see e.g. [37],

$$\sigma^a[\bar{g}; g] = (\bar{s} - s) \frac{d\lambda^a}{ds}(\bar{s}) \quad (4)$$

This construction is illustrated in Figure 1. The geodesics  $\lambda(s)$  are taken with respect to Vilkovisky's connection and satisfy  $\lambda(\bar{s}) = \bar{g}$  and  $\lambda(s) = g$ , and  $s$  is the affine parameter of the geodesic. Heuristically speaking, Vilkovisky's connection is designed to maximally disentangle the fibre from the base space. It is defined through its Christoffel symbols

$$\Gamma_V^i{}_{jk} = \Gamma_\gamma^i{}_{jk} - Q^i{}_{\alpha(j} \omega^{\alpha}{}_{k)} + \frac{1}{2} \omega^\alpha{}_{(j} Q^i{}_{\alpha l} Q^l{}_{\beta} \omega^{\beta}{}_{k)} \quad (5)$$

where  $\Gamma_\gamma$  are the Christoffel symbols of the Riemannian connection induced by the supermetric  $\gamma$  and  $Q_\alpha$  are the generators of the diffeomorphism group. The  $\omega^\alpha{}_i$  are

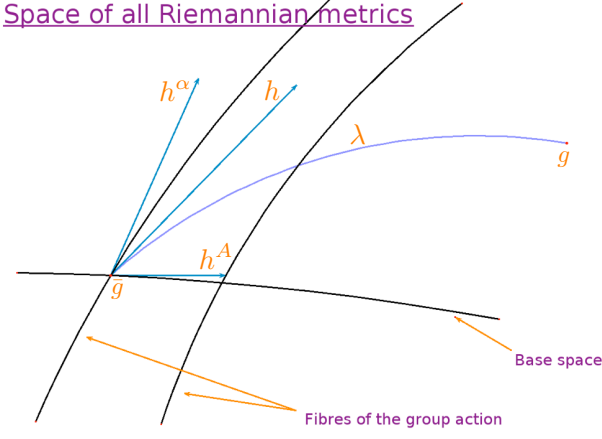


FIG. 1: Geodesic w.r.t. the Vilkovisky connection from  $\bar{g}$  to  $g$ .  $\sigma$  is the tangent vector at  $\bar{g}$  on this geodesic,  $h^A$  is the diffeomorphism-invariant projection, and  $h^\alpha$  the projection on the diffeomorphism fibre.

the components of the unique connection one-form  $\omega^\alpha$  determined by  $\gamma$  and  $Q_\alpha$ , i.e.

$$\omega^\alpha = \mathfrak{G}^{\alpha\beta} \gamma(Q_\beta, \cdot) \quad (6)$$

where  $\mathfrak{G}^{\alpha\beta}$  stands for the inverse operator of  $-\gamma(Q_\alpha, Q_\beta)$ . With DeWitt's condensed notation the index  $i = (x, \mu)$  labels space-time  $x$  and Lorentz indices  $\mu$ . Additionally, the subscripts  $\cdot j$  denote covariant derivatives with respect to  $\Gamma_\gamma$  and the parenthesis in the subscripts indicate symmetrization of the indices embraced. More details in the context of functional RG flows in the geometrical approach can be found in [9, 31–33].

The above geometrical construction allows us to define the path integral of the theory in a manifestly reparametrisation invariant way

$$e^{-\hat{\Gamma}[\bar{g}; h]} = \int \mathcal{D}g \sqrt{\det \gamma} \delta(\mathcal{F}) \det M[\bar{g}; g] \times \exp \left\{ -S[g] - \int \frac{\delta \hat{\Gamma}}{\delta h} \cdot (\sigma[\bar{g}; g] + h) \right\}. \quad (7)$$

Here  $\mathcal{D}g \sqrt{\det \gamma}$  stands for the volume form on  $\Phi$ ,  $\mathcal{F} = 0$  is the gauge fixing condition and  $\det M$  is the determinant of the ghost operator which depends both on the background  $\bar{g}$  and the fluctuating field. We emphasise that the gauge fixing is only introduced for the sake of convenience: the effective action  $\hat{\Gamma}$  does not depend on it. This goes hand in hand with the fact that the geometrical effective action  $\hat{\Gamma}$  in (7) only depends on the diffeomorphism-invariant part  $h^A$  of the field  $h$  with coordinates  $h^\alpha = (h^A, h^\alpha)$ ,

$$h^\alpha = -\sigma^\alpha[\bar{g}; g], \quad h^A = (\Pi h)^A, \quad h^\alpha = ((1 - \Pi)h)^\alpha. \quad (8)$$

Here we have introduced the horizontal projection operator  $\Pi = \Pi(\bar{g})$  on the diffeomorphism-invariant part of  $h$ , see e.g. [9, 32, 37]. The part of the geodesic normal field tangential to the fibre,  $h^\alpha$ , drops out. Note also, that in the linear approximation,  $h$  is equivalent with the metric fluctuation  $g - \bar{g}$  in the background field approach,  $h = g - \bar{g} + O(h^2)$ . With these prerequisites it is possible to rewrite the path integral in (7) in terms of the field  $h$

$$e^{-\Gamma[\bar{g}; h]} = \int \mathcal{D}h^A \sqrt{\det \gamma^{AB}} e^{-S[\bar{g}; \hat{h}]} \int \mathcal{D}\hat{h}^\alpha \sqrt{\det \gamma^{\alpha\beta}} \times e^{-S_{\text{gf}}[\bar{g}; h]} \det^{1/2} \mathcal{F}^2 \det M e^{\int \frac{\delta \Gamma}{\delta h} \cdot (\hat{h} - h)}, \quad (9)$$

where  $\mathcal{F}^2$  is the distribution kernel of the gauge fixing term  $S_{\text{gf}}$ ,

$$S_{\text{gf}}[\bar{g}; h] = \frac{\kappa^2}{\alpha} \int d^d x \sqrt{\bar{g}} \bar{g}^{\mu\nu} \mathcal{F}_\mu \mathcal{F}_\nu, \quad (10)$$

with  $\kappa$  defined as in (2). We emphasise that the Gaussian integration over the fibre field  $\hat{h}^\alpha$  in (9) is only kept for the sake of convenience. Performing it would make explicit that the effective action  $\Gamma[\bar{g}; h]$  defined in (9) only depends on  $h^A$  up to the gauge fixing term,

$$\Gamma[\bar{g}; h] = \hat{\Gamma}[\bar{g}; h^A] + S_{\text{gf}}[\bar{g}; h]. \quad (11)$$

In the following we impose a linear gauge fixing condition

$$\mathcal{F}_\tau = F_\tau^{\mu\nu}[\bar{g}] \hat{h}_{\mu\nu} = 0. \quad (12)$$

with a linear operator  $F_\tau^{\mu\nu}[\bar{g}]$  which depends on the background  $\bar{g}$ . In this case the ghost operator  $M$  in (9) depends solely on the background field configuration  $\bar{g}$  but not on the fluctuating field  $\hat{h}$ . Put intuitively,  $\det M$  accounts for the fact that the gauge fixing surface specified by  $\mathcal{F}$  intersects each gauge orbit at a different angle. In general the intersection angle will depend on the dynamical field configuration  $g$  parametrizing the orbit, see (7). Note, however, that the path integral in (9) is taken over a linear manifold and the gauge orbits are linear hypersurfaces – the vertical subspaces spanned by the  $h^\alpha$  coordinates. Then, with (12) it is clear that the gauge fixing surface will intersect each orbit at the same angle leading to a constant  $M$ .

It is convenient though not necessary to choose the gauge fixing such that  $h^A$  satisfies (12), see e.g. [32]. With (8) this amounts to  $F \cdot \Pi = 0$ . Then it is evident that the Gaussian integration over  $h^\alpha$  drops out, leading to purely background field dependent terms multiplied by  $\det \gamma^{\alpha\beta}$ . Nonetheless it turns out to be convenient to keep the gauge fixing term and use it in order to facilitate computations. Specifically we choose

$$F_\tau^{\mu\nu}[\bar{g}] = \gamma^{\mu\nu\rho'\sigma'}[\bar{g}] Q_{\rho'\sigma',\tau}[\bar{g}] \quad (13)$$

Using the well-known expression for the generators of the diffeomorphism group

$$Q^i_\alpha[\bar{g}] = Q_{\tau}^{\rho'\sigma'}[\bar{g}] = -\delta_{\tau}^{\rho'} \bar{\nabla}^{\sigma'} - \delta_{\tau}^{\sigma'} \bar{\nabla}^{\rho'} \quad (14)$$

we obtain

$$F_\tau^{\mu\nu}[\bar{g}] = -2 \left( \delta_\tau^{(\mu} \bar{\nabla}^{\nu)} + \frac{1}{2} \theta \bar{g}^{\mu\nu} \bar{\nabla}_\tau \right). \quad (15)$$

Here,  $\bar{\nabla}$  is the covariant derivative with respect to the background metric connection. It is now straightforward to show that

$$S_{\text{gf}} = -\frac{\kappa^2}{\alpha} \int d^d x \sqrt{\bar{g}} \hat{h}_{\mu\nu} \left( \bar{g}^{\mu\sigma'} \bar{\nabla}^\nu \bar{\nabla}^{\rho'} + \theta \bar{g}^{\mu\nu} \bar{\nabla}^{\rho'} \bar{\nabla}^{\sigma'} + \frac{1}{4} \theta^2 \bar{g}^{\mu\nu} \bar{g}^{\rho'\sigma'} \bar{\Delta} \right) \hat{h}_{\rho'\sigma'}, \quad (16)$$

with  $\alpha$  being the gauge-fixing parameter and  $\bar{\Delta} \equiv \Delta_{\bar{g}}$  the Laplace operator constructed from the background metric. Finally we discuss the  $\sqrt{\det \gamma}$ -terms in (9), for details see e.g. [37]. First of all we note that the full metric  $\gamma$  does not depend on the  $h^\alpha$  due to the vanishing Lie-derivative  $\mathcal{L}_{Q_\alpha} \gamma = 0$ . The horizontal part  $\gamma^{AB}$  does not depend on the  $h^A$  either which leaves  $\gamma^{\alpha\beta}$  as the only dynamical object. Explicitly it reads

$$\gamma^{\alpha\beta} = \left( 2\delta_\nu^\mu \Delta + 2R_\nu^\mu + 2(1+\theta) \nabla^\mu \nabla_\nu \right) \delta(x, x') \quad (17)$$

with  $\alpha = (\mu, x)$  and  $\beta = (\nu, x')$ . The determinant of  $\gamma^{\alpha\beta}$  can be rewritten in terms of a Grassmann integral,

$$\begin{aligned} \det \gamma^{\alpha\beta}[\bar{g}, h^A] & \quad (18) \\ &= \int D\bar{c} Dc e^{\int d^d x \sqrt{\bar{g}} \bar{c}_\mu \left( 2\delta_\nu^\mu \Delta + 2R_\nu^\mu + 2(1+\theta) \nabla^\mu \nabla_\nu \right) c^\nu}. \end{aligned}$$

Here  $c(x)$  and  $\bar{c}(x)$  are anti-commuting Grassmann fields and  $g$  is a metric with  $-\sigma^A[\bar{g}, g] = h^A$ . Eq.(18) can most easily be understood as the geometric analogue of the usual ghost action. This leaves us with the final expression for the geometrical effective action,

$$\begin{aligned} e^{-\Gamma[\bar{g}; h]} &= \int \mathcal{D}\hat{h}^A \sqrt{\det \gamma^{AB}} \int \mathcal{D}\hat{h}^\alpha \int D\bar{c} Dc \\ &\times e^{-S[\bar{g}; \hat{h}, c, \bar{c}]} \det^{1/2} \mathcal{F}^2 \det M e^{\int \frac{\delta \Gamma}{\delta h} \cdot (\hat{h} - h)}, \quad (19) \end{aligned}$$

where the remaining measure factors of the path integral only lead to background-dependent terms and  $S[\bar{g}; \hat{h}, c, \bar{c}]$  is the full gauge-fixed action,

$$\begin{aligned} S[\bar{g}; \hat{h}, c, \bar{c}] &= 2\kappa^2 \int d^d x \sqrt{\bar{g}} \left( -R(g) + 2\bar{\Delta}_k \right) + S_{\text{gf}} \\ &+ 2 \int d^d x \sqrt{\bar{g}} \bar{C}_\mu \left( \delta_\nu^\mu \Delta + R_\nu^\mu + (1+\theta) \nabla^\mu \nabla_\nu \right) C^\nu. \quad (20) \end{aligned}$$

We emphasise again that even though the path integral (19) is defined similarly to the standard gauge-fixed approach, the effective action  $\Gamma - S_{\text{gf}}$  does not depend on the gauge fixing.

### III. GEOMETRICAL RG-FLOWS

The geometrical approach put forward in the last section allows for a diffeomorphism-invariant infrared regularisation as the dynamical field  $h^A$  is diffeomorphism-invariant. Flow equations for the geometrical effective action have first been put forward in [31] for the sharp-cutoff and in [32] for general regulators. The approach has been put to work in the Einstein-Hilbert approximation in [33]. In [32] it has been shown that, despite manifest diffeomorphism or gauge invariance, the approach is subject to non-trivial, regulator-dependent Nielsen identities. Heuristically speaking, these identities carry the information about the unitarity of the theory. This interesting and important relation will be discussed elsewhere.

A diffeomorphism-invariant infrared regularisation can now be applied to the theory by modifying the propagation of the fluctuation fields through the substitution  $S[\bar{g}; \hat{h}, c, \bar{c}] \rightarrow S[\bar{g}; \hat{h}, c, \bar{c}] + \Delta S_k[\bar{g}; \hat{h}, c, \bar{c}]$  with the cut-off term

$$\begin{aligned} \Delta S_k[\bar{g}; \hat{h}, \bar{c}, c] &= \frac{1}{2} \int d^d x \sqrt{\bar{g}} \hat{h}_{\mu\nu} \mathcal{R}_k^{\mu\nu\rho\sigma}[\bar{g}] \hat{h}_{\rho\sigma} \\ &+ \int d^d x \sqrt{\bar{g}} \bar{c}_\mu \mathcal{R}_k^{\mu\nu}[\bar{g}] c_\nu. \quad (21) \end{aligned}$$

Note that the regulators  $\mathcal{R}_k^{\mu\nu\rho\sigma}$  and  $\mathcal{R}_k^{\mu\nu}$  only depend on the background field configuration. For convenience, we further demand that  $\mathcal{R}_k^{\mu\nu\rho\sigma}$  should satisfy  $\mathcal{R}_{k, \alpha A} = \mathcal{R}_{k, A\alpha} = 0$ , see [32]. This disentangles the trivial flow of the  $h^\alpha$ -part of the action from the dynamical flow of the  $h^A$ -part. Inserting the regulator terms into the path integral (19) we are led to the Wetterich equation for quantum gravity within the geometrical approach,

$$\partial_t \Gamma_k[\bar{g}; \phi] = \frac{1}{2} \text{Tr} \frac{1}{\Gamma_k^{(2)}[\bar{g}; \phi] + \mathcal{R}_k[\bar{g}]} \partial_t \mathcal{R}_k[\bar{g}], \quad (22)$$

where the trace sums over momenta, internal indices and all field species with a relative minus sign for Grassmann fields. The super-field  $\phi = (h, C, \bar{C})$  contains all fluctuation fields. The components are the expectation values of the dynamical fields, i.e.

$$h = \langle \hat{h} \rangle \quad C_\mu = \langle c_\mu \rangle, \quad \bar{C}_\mu = \langle \bar{c}_\mu \rangle. \quad (23)$$

and the two-point function  $\Gamma_k^{(2)}[\bar{g}; \phi]$  is the second derivative of the effective action  $\Gamma$  w.r.t. the field  $\phi$ ,

$$\Gamma_k^{(2)}[\bar{g}; \phi] = \frac{\delta^2 \Gamma_k}{\delta \phi_i \delta \phi_j}. \quad (24)$$

The regulator  $\mathcal{R}_k$  is diagonal in superfield space with diagonal components

$$\mathcal{R}_{k, hh} = (\mathcal{R}_k^{\mu\nu\rho\sigma}), \quad \mathcal{R}_{k, C\bar{C}} = (\mathcal{R}_k^{\mu\nu}) = -(\mathcal{R}_k^{\nu\mu}). \quad (25)$$

As can be immediately inferred from the construction of the geometrical effective action, we also have in general

$$\frac{\delta \partial_t \Gamma_k[\bar{g}; \phi]}{\delta \phi} = \frac{\delta \partial_t \hat{\Gamma}_k[\bar{g}; \phi]}{\delta \phi}, \quad (26)$$

i.e. the flows of  $\hat{\Gamma}_k$  and  $\Gamma_k$  agree up to normalisation factors that might depend on the background metric. In particular this entails that the gauge fixing term does not flow. Ultimately we are interested in the evolution of  $\Gamma_k[\bar{g}; 0]$  with the cut-off scale  $k$ . In this case the propagator on the right hand side of (22) can be rewritten as

$$\Gamma_k^{(2)}[\bar{g}; h = 0] = \nabla^2 \hat{\Gamma}_k[\bar{g}, g = \bar{g}] + S_{\text{gf}}^{(2)}. \quad (27)$$

In (27) we have used that  $h = -\sigma[\bar{g}; g]$ . The second covariant derivative  $\nabla^2$ , taken with respect to  $\Gamma^V$ , acts on the full dynamical metric field  $g$ . For notational convenience we omitted the ghost fields. Note that within the standard background field approach (27) simply reads

$$\Gamma_k^{(2)}[\bar{g}; h = 0] = \frac{\Gamma_k[\bar{g}; g = \bar{g}]}{\delta g^2}. \quad (28)$$

The symmetric tensor  $h$  can be further decomposed with the York transverse-traceless decomposition valid for spherical background geometries. This decomposition together with that of the ghosts is detailed in Appendix A. In the present work all diagonal modes  $\phi_i$  are regularised with regulators

$$\mathcal{R}_{k,i} = \mathcal{T}_i k^2 r(x), \quad \text{with} \quad x = -\frac{\Delta \bar{g}}{k^2}. \quad (29)$$

where  $r(x)$  is a dimensional shape function and the prefactor  $\mathcal{T}_i$  accounts for the tensorial structure of the respective mode. The complete list of regulators can be found in Appendix D.

We close this section with a discussion of the practical implementation of the flow (22) in the graviton sector in a given approximation. This repeats the discussion concerning the trivial difference between the diffeomorphism-invariant effective action, here  $\hat{\Gamma}_k$ , and the trivially gauge-fixed effective action, here  $\Gamma_k = \hat{\Gamma}_k + S_{\text{gf}}$ , in the context of the flow equation. The general derivations are done in detail in [32].

Approximations or parameterisations of the effective action  $\Gamma_k$  contain a diffeomorphism-invariant functional of  $g$  such as the Einstein-Hilbert action. This functional has to be accompanied by terms which preserve symmetry constraints such as the Nielsen identities. The flow depends on the second derivative of  $\Gamma_k$  w.r.t.  $h$  which has to be extracted from the action. For functionals of  $g$  this amounts to taking second derivatives w.r.t. Vilkovisky's connection. Here we discuss how this task can be reduced to computing Riemannian covariant derivatives at  $g = \bar{g}$ . Separating the graviton and ghost contributions

and identifying  $g = \bar{g}$ , the flow reads with (11)

$$\begin{aligned} \partial_t \Gamma_k &= \frac{1}{2} \text{Tr} \frac{1}{\nabla^2 \hat{\Gamma}_k + S_{\text{gf}}^{(2)} + \mathcal{R}_k^{\text{grav}}} \partial_t \mathcal{R}_k^{\text{grav}} \\ &+ \text{ghost} - \text{contr.} \end{aligned} \quad (30)$$

Since  $\hat{\Gamma}_k$  is a diffeomorphism-invariant functional, the covariant derivative  $\hat{\Gamma}_k^{(2)} = \nabla^2 \Gamma_k$  has only a transversal part. If we choose a purely transversal regulator  $\mathcal{R}_k^{\text{grav}}[\bar{g}]$ , i.e.

$$\mathcal{R}_k^{\text{grav}}[\bar{g}] = \left( \begin{array}{c|c} \mathcal{R}_{k,\perp}^{\text{grav}}[\bar{g}] & 0 \\ \hline 0 & 0 \end{array} \right), \quad (31)$$

the term  $S_{\text{gf}}^{(2)}$  drops out from the flow. This entails that the geometrical flow cannot depend on the gauge fixing, for the general argument see [32]. Thus, we could as well work solely with  $\hat{\Gamma}_k$  and its propagator. However, for practical computations it turns out to be more convenient to invert the propagator on the full transversal + longitudinal space, hence using  $\Gamma_k$  instead of  $\hat{\Gamma}_k$ . It is also here where we make use of the crucial identity (47). Schematically we have at  $g = \bar{g}$ ,

$$\nabla^2 \hat{\Gamma}_k = \Pi[\bar{g}] \cdot \nabla_\gamma^2 \hat{\Gamma}_k[\bar{g}] \cdot \Pi[\bar{g}] \quad (32)$$

see (8). With  $F \cdot \Pi[\bar{g}] = 0$  and (12) the gauge-fixing term has the form

$$S_{\text{gf}}^{(2)}[\bar{g}] = -\frac{\kappa^2}{\alpha} \left( \begin{array}{c|c} -\frac{0}{0} & \frac{0}{\mathcal{F} \cdot \mathcal{F}} \\ \hline & \end{array} \right), \quad (33)$$

It is proportional to  $1/\alpha$  and diverges for  $\alpha \rightarrow 0$ . We also introduce a corresponding longitudinal part to the regulator

$$\mathcal{R}_k^{\text{grav}}[\bar{g}] = \left( \begin{array}{c|c} \mathcal{R}_{k,\perp}^{\text{grav}}[\bar{g}] & 0 \\ \hline 0 & \mathcal{R}_{k,L}^{\text{grav}}[\bar{g}] \end{array} \right). \quad (34)$$

This modification adds a trivial  $\bar{g}$ -dependent part to the flow, see also (26). Note also that even though  $\Gamma_k$  is a diffeomorphism-invariant functional, its covariant derivative with respect to the metric connection is not. This is taken into account by writing schematically

$$\nabla_\gamma^2 \hat{\Gamma}_k = \left( \begin{array}{c|c} \nabla^2 \hat{\Gamma}_k & B \\ \hline C & D \end{array} \right) \quad (35)$$

where the subscript  $\gamma$  indicates that the covariant derivative is taken with respect to the metric rather than the Vilkovisky connection. Now we consider

$$\begin{aligned} &\nabla_\gamma^2 \hat{\Gamma}_k + S_{\text{gf}}^{(2)} + \mathcal{R}_k^{\text{grav}} \\ &= \left( \begin{array}{c|c} \nabla^2 \hat{\Gamma}_k + \mathcal{R}_{k,\perp}^{\text{grav}}[\bar{g}] & B \\ \hline C & D + \mathcal{R}_{k,L}^{\text{grav}} + S_{\text{gf}}^{(2)} \end{array} \right), \end{aligned} \quad (36)$$

in a slight abuse of notation, where  $T$  is completely longitudinal. This applies to the gauge fixing term,  $S_{\text{gf}}^{(2)}$  in (33), and to a sum of gauge fixing term and longitudinal regulator as introduced in (34). In these cases we have

$$\lim_{\alpha \rightarrow 0} \left( \begin{array}{c|c} \nabla^2 \hat{\Gamma}_k + \mathcal{R}_{k,\perp}^{\text{grav}} & B \\ \hline C & D + \mathcal{R}_{k,L}^{\text{grav}} + S_{\text{gf}}^{(2)} \end{array} \right)^{-1} = \left( \begin{array}{c|c} \Pi \cdot \frac{1}{\nabla^2 \hat{\Gamma}_k + \mathcal{R}_{k,\perp}^{\text{grav}}} \cdot \Pi & 0 \\ \hline 0 & 0 \end{array} \right) \quad (37)$$

where, as before, the  $\pi$ 's indicate that we are inverting on the transversal subspace. In summary we can rewrite the right hand side of eq.(22) at  $g = \bar{g}$  in the form

$$\lim_{\alpha \rightarrow 0} \frac{1}{2} \text{Tr} \frac{1}{\nabla_\gamma^2 \hat{\Gamma}_k[\bar{g}] + S_{\text{gf}}^{(2)}[\bar{g}] + \mathcal{R}_k^{\text{grav}}[\bar{g}]} \partial_t \mathcal{R}_k^{\text{grav}}[\bar{g}] - \text{Tr} \frac{1}{-\mathcal{Q}[\bar{g}] + \mathcal{R}_k^{\text{gh}}[\bar{g}]} \partial_t \mathcal{R}_k^{\text{gh}}[\bar{g}]. \quad (38)$$

Eq. (38) entails the reduction of the propagator in terms of covariant derivatives w.r.t. Vilkovisky's connection to an expression which depends on Riemannian covariant derivatives. The price to pay is the intermediate introduction of a gauge fixing, which, however, does not play a role in the final expression.

#### IV. APPROXIMATION

The standard Einstein-Hilbert truncation in the background field approach to quantum gravity amounts to introducing a flowing cosmological constant and Newton constant into the full, gauge-fixed Einstein-Hilbert action, (20), that is

$$\Gamma_{\text{EH}}[\bar{g}; \phi] = 2\kappa^2 \bar{Z}_{N,k} \int d^d x \sqrt{\bar{g}} (-R(g) + 2\bar{\Lambda}_k) + S_{\text{gf}} + 2 \int d^d x \sqrt{\bar{g}} \bar{C}_\mu \left( \delta_\nu^\mu \Delta + R_\nu^\mu + (1 + \theta) \nabla^\mu \nabla_\nu \right) C^\nu, \quad (39)$$

where  $\kappa^2$  is defined in (2), and  $\hat{\Gamma}_{\text{EH}} = \Gamma_{\text{EH}} + S_{\text{gf}}$ . As before  $h = -\sigma[\bar{g}; g]$  and all geometric quantities such as  $\Delta$ ,  $R_\nu^\mu$  and  $\nabla^\mu$  are constructed with respect to the full metric  $g$ . The cut-off dependent quantities  $\bar{Z}_{N,k}$  and  $\bar{\Lambda}_k$  stand for the scale-dependent wavefunction renormalisation factor and the scale-dependent cosmological constant respectively. At vanishing fluctuation field  $h = 0$  (39) solely depends on the full metric  $g = \bar{g}$  and is diffeomorphism-invariant. At  $h \neq 0$  it is still diffeomorphism-invariant w.r.t. a combined transformation of  $\bar{g}$  and  $h$ . However, the approximation (39) does not respect the Nielsen identity, [9, 32]. This is discussed in detail in the next Section V.

Here we simply anticipate the occurrence of further terms due to the Nielsen identity and introduce an extended Einstein-Hilbert truncation,

$$\Gamma_k[\bar{g}; h, \bar{C}, C] = \Gamma_{\text{EH}}[g; \bar{C}, C] + \Delta\Gamma[\bar{g}; h] + \text{higher order}. \quad (40)$$

with

$$\Delta\Gamma[\bar{g}; 0] = 0, \quad (41)$$

The higher order terms stand for additional diffeomorphism-invariant terms in the full metric  $g$ , and the ghost part of the action is the same as in eq.(39). The Einstein-Hilbert term depends on the full metric  $g$  whereas  $\Delta\Gamma[\bar{g}; h]$  stands for quantum fluctuations that depend on the fluctuations  $h$  and the background  $\bar{g}$  separately. In the minimally consistent completion of the Einstein-Hilbert truncation  $\Delta\Gamma$  contains a 'mass' term for the fluctuation field  $h$  and a contribution to the kinetic term for  $h$ . In DeWitt's condensed notation the decomposition has the form

$$\Delta\Gamma[\bar{g}; h] = \Delta\Gamma_1 + \Delta\Gamma_2 = \Delta\Gamma^a h_a + \frac{1}{2} \Delta\Gamma^{ab} h_a h_b, \quad (42)$$

with symmetric coefficients  $\Delta\Gamma_{ab} = \Delta\Gamma_{ba}$ . The term  $\Delta\Gamma_1$  is linear in  $h$  and reads

$$\Delta\Gamma_1[\bar{g}; h] = \int d^d x \sqrt{\bar{g}} \Delta\Gamma^{\mu\nu}[g] h_{\mu\nu}. \quad (43)$$

whereas  $\Delta\Gamma_2$  is quadratic in  $h$  with

$$\Delta\Gamma_2 = \frac{1}{2} \int d^d x \sqrt{\bar{g}} h_{\mu\nu} \Delta\Gamma^{\mu\nu\rho\sigma}[g] h_{\rho\sigma}. \quad (44)$$

Here we dropped terms of order higher than  $h^2$  with  $g$ -dependent expansion coefficients  $\Delta\Gamma^{a_1 \dots a_n}$ . Due to diffeomorphism invariance the expansion coefficients can only couple to the  $h_A$ , the fibre variables  $h_\alpha$  have to drop out. Consequently  $\Delta\Gamma^a$  and  $\Delta\Gamma^{ab}$  have to be proportional to  $\Pi$ . The input in the flow equation is the second  $h$ -derivative of  $\Delta\Gamma$ . For  $h = 0$ , that is  $g = \bar{g}$ , it reads schematically

$$\Delta\Gamma^{(2)}[g] = \Delta\Gamma_{a,b} + \Delta\Gamma_{b,a} + \Delta\Gamma_{ab}, \quad (45)$$

where the first two terms on the rhs arise from  $\Delta\Gamma_1$ , and the last term on the rhs comes from  $\Delta\Gamma_2$ . The distribution kernel of the second order term is specified with

$$\Delta\Gamma^{(2)}[g] = 4\kappa^2 (Z_N \Lambda_k - \bar{Z}_N \bar{\Lambda}_k) T_\Lambda + 2\kappa^2 (Z_N - \bar{Z}_N) T_N. \quad (46)$$

The  $T_\Lambda$  and  $T_N$  stand for the tensor structures arising from the second variation w.r.t.  $g$  of the cosmological constant term and the curvature term in the Einstein-Hilbert action in (40). The term (46) involves two new flowing coefficients  $Z_{N,k}$  and  $\Lambda_k$ . Due to (45),  $\Delta\Gamma^{(2)}[g]$  has contributions both from  $\Delta\Gamma_1$  and  $\Delta\Gamma_2$ . With the tensor structure defined by  $T_\Lambda$  and  $T_N$ , (46) projects onto the diffeomorphism-invariant variables  $h_A$  as demanded by diffeomorphism invariance.

Note also that the above approximation includes an Einstein-Hilbert term  $\Gamma_{\text{EH}}[\bar{g}] = \Gamma_{\text{EH}}[\bar{g}; 0]$ . Such a term can be expanded about the full metric,  $\bar{g} = g - h + O(h^2)$  and is absorbed in the Einstein Hilbert term as well as in  $\Delta\Gamma$ . Schematically the expansion of  $\Gamma_{\text{EH}}[\bar{g}]$  reads

$$\begin{aligned}\Gamma_{\text{EH}}[g - h + O(h^2)] &= \Gamma_{\text{EH}}[g] + \Gamma_{\text{EH},a}[g]h^a + O(h^2) \\ &= \Gamma_{\text{EH}}[\bar{g}] + \Gamma_{\text{EH},a}[\bar{g}]h^a + O(h^2).\end{aligned}$$

In the same spirit it was possible to introduce a single metric dependence in  $\sqrt{\bar{g}}\Delta\Gamma^{\mu\nu\rho\sigma}[g]$  in (42). Differences in  $\bar{g}$  and  $g$  are absorbed in terms of order higher than two in  $h$ . The latter are not taken into account in the present approximation.

In summary, the minimally consistent Einstein-Hilbert approximation leads to the following identity for the second derivative of the effective action w.r.t.  $h$ ,

$$\Gamma_{k,ab}[\bar{g}, 0] = \left( \hat{\Gamma}_{\text{EH}} \right)_{,cd} [\bar{g}] \Pi^c_a \Pi^d_b \Big|_{\bar{\Lambda} \rightarrow \Lambda, \bar{Z}_N \rightarrow Z_N} + S_{\text{gf}}^{(2)}, \quad (47)$$

see (8), (40) and (42). This leaves us with the task to compute  $\nabla_\gamma^2 \hat{\Gamma}_{\text{EH}} + S_{\text{gf}}^{(2)}$  at  $g = \bar{g}$ . The results are listed in Appendix B. The propagator on the right hand side of the flow equation (22) depends on  $\Gamma_{k,ab}$  and hence only on  $(\Lambda, Z_N)$ . The standard background field approximation in the geometrical approach amounts to

$$(\Lambda, Z_N) = (\bar{\Lambda}, \bar{Z}_N), \quad (48)$$

in (47). In other words, the additional term  $\Delta\Gamma$  simply compensates for the fact that the propagator of the fluctuation field does not depend on the background parameters  $\bar{Z}_N, \bar{\Lambda}$  but on the fluctuation parameters  $Z_N, \Lambda$ .

We summarise the flow equation in the approximation introduced above as follows: we have a coupled set of differential equations for the dimensionless pair  $(g_N, \lambda)$  of dynamical couplings with

$$g_N = \frac{k^{d-2}G_N}{Z_{N,k}}, \quad \lambda = k^{-2}\Lambda_k, \quad \eta_N = -\frac{\partial_t Z_{N,k}}{Z_{N,k}}, \quad (49)$$

leading to

$$\eta_N = \frac{\partial_t g_N + (2-d)g_N}{g_N}. \quad (50)$$

With the definitions in (49) we have

$$\partial_t g_N + (2-d)g_N = F_g(g_N, \lambda), \quad (51a)$$

$$\partial_t \lambda + (2-\eta_N)\lambda = F_\lambda(g_N, \lambda). \quad (51b)$$

The set of flow equations (50) does not depend on the background couplings  $(\bar{g}_N, \bar{\lambda})$  defined analogously to (49)

$$\bar{g}_N = \frac{k^{d-2}\bar{G}_N}{Z_{N,k}}, \quad \bar{\lambda} = k^{-2}\bar{\Lambda}_k, \quad \bar{\eta}_N = -\frac{\partial_t \bar{Z}_{N,k}}{\bar{Z}_{N,k}}. \quad (52)$$

This fact reflects the background independence of the approach. In turn, the flows (51) induce flows for the dimensionless pair  $(\bar{g}_N, \bar{\lambda})$

$$\frac{g_N}{\bar{g}_N} (\partial_t \bar{g}_N + (2-d)\bar{g}_N) = \bar{F}_g(g_N, \lambda), \quad (53a)$$

$$\frac{g_N}{\bar{g}_N} (\partial_t \bar{\lambda} + (2-\bar{\eta}_N)\bar{\lambda}) = \bar{F}_\lambda(g_N, \lambda). \quad (53b)$$

Note that the right-hand sides in (53) do not depend on  $\bar{g}_N, \bar{\lambda}$ , and thus the flow of the background couplings  $(\bar{Z}_N, \bar{\Lambda})$  only depends on the dynamical couplings  $(Z_N, \Lambda)$ . The ratios  $g_N/\bar{g}_N$  on the lhs of (53) simply originate from using the Newton constants  $g_N, \bar{g}_N$  instead of  $Z_N, \bar{Z}_N$ .

In the background field approximation, (47), the system of flows (51),(53) is substituted by (53) with  $g_N = \bar{g}_N$  and  $\lambda = \bar{\lambda}$ . In this case the ratio is unity and we arrive at a coupled set of two flow equations for  $g_N$  and  $\lambda$  very similar to the standard background flows, see Section VI. The only difference is the appearance of the covariant derivatives in the propagator. In the present work we shall also solve the full system (51),(53). This is done in the Sections VIII, IX.

We close this section with a discussion of observables. In the background field approach only the correlation functions of the background metric are diffeomorphism-covariant and can be directly used to construct observables such as cross-sections. In the present approach the corresponding correlation functions depend on to the running Newton constant  $\bar{g}_N$  and the running cosmological constant  $\bar{\lambda}_N$ . In the geometrical approach also the dynamical couplings  $g_N$  and  $\lambda$  are coefficients of diffeomorphism-invariant terms. However, the background couplings comprise *local* information about the theory whereas the dynamical couplings do not. A direct physics interpretation has to be taken with caution. Note, however, that the fixed points of the theory are signaled by vanishing  $\beta$ -functions of the dynamical couplings.

## V. NIELSEN IDENTITIES

For the computation of  $\Delta\Gamma$  we shall resolve the difference between the background metric and the full metric in a leading order approximation. To that end we first discuss the usual background field approach, where  $g = \bar{g} + h$ . This relates to the linear approximation in the geometrical approach. Note, however, that the effective action is not a function of  $g$  but of  $\bar{g}$  and  $h$  separately. The standard approximation used in background field flows is done by evaluating the flow (22) at vanishing  $h = 0$ . Then, the flow is a flow for  $\Gamma_k[\bar{g}; 0]$ . It is not closed as the right hand side of (22) depends on  $\Gamma_k^{(2)}$ , the second derivative of the scale-dependent effective action

w.r.t. the fluctuation field  $h$ . The approximation

$$\frac{\delta^2 \Gamma_k}{\delta h^2} [\bar{g}; 0] = \frac{\delta^2 \Gamma_k}{\delta \bar{g}^2} [\bar{g}; 0], \quad (54)$$

closes the flow (22) in the linear approximation. The identity (54) is violated by the fact that the effective action is not a function of  $\bar{g} + h$ , but of both fields separately. The truncation (54) fails already at one loop in the standard background field approach. Hence a computation of the flow of  $\Gamma_k[\bar{g}, 0]$  with (54) deviates from the full flow already at two loop [41–44], for infrared diverging regulators it even fails at one loop [43]. In [41] the difference to the correct one loop result for  $\Gamma_k^{(2)}$  was used for deriving the two loop  $\beta$ -function in Yang-Mills theory. Using the fluctuating propagators in the flow is also crucial for deriving confinement within Landau gauge QCD, see [45]. Indeed, generally derivatives w.r.t.  $g$  (or  $h$ ) and that w.r.t.  $\bar{g}$  are related by Nielsen identities [9, 32]. Within the geometrical approach used in the present work they read

$$\Gamma_{k,i} + \Gamma_{k,a} \langle \hat{h}^a ; i \rangle = \frac{1}{2} G^{ab} \mathcal{R}_{ba,i} + \mathcal{R}_{ab} G^{bc} \frac{\delta}{\delta \bar{h}^c} \langle \hat{h}^a ; i \rangle. \quad (55)$$

The subscript  $,i$  stands for the usual derivative and  $;i$  for the  $\Gamma_V$ -covariant derivative acting on the background metric  $\bar{g}$ . The index  $a$  indicates differentiation with respect to the Gaussian normal coordinate  $h^a$  and  $G$  stands for the full propagator. Eq. (55) entails that, up to regulator effects, derivatives w.r.t. the background metric are indeed proportional to those w.r.t. geodesic normal fields  $h$  as opposed to the corresponding identities in the standard background field approach, see [9, 41, 43].

The proportionality factor  $\langle \hat{h}^a ; i \rangle$  is sensitive to quantum effects and encodes the quantum deformation of diffeomorphism invariance in a similar way as the BRST master equation encodes the quantum deformation of classical BRST invariance [9, 32]. Inserting the Einstein-Hilbert truncation (40) in the Nielsen identity (55) we are led to

$$\begin{aligned} \Gamma_{\text{EH},a} \left( \langle \hat{h}^a ; i \rangle - h^a ; i \right) &+ \left( \Delta \Gamma_{k,i} + \Delta \Gamma_{k,a} \langle \hat{h}^a ; i \rangle \right) \\ &= \frac{1}{2} G^{ab} \mathcal{R}_{ba,i} + \mathcal{R}_{ab} G^{bc} \frac{\delta}{\delta \bar{h}^c} \langle \hat{h}^a ; i \rangle. \end{aligned} \quad (56)$$

In (56) we have used that the Einstein-Hilbert action  $\Gamma_{\text{EH}}$  satisfies the classical Nielsen identity, that is (55) with vanishing right hand side and  $\langle \hat{h}^a ; i \rangle \rightarrow h^a ; i$ . This entails that (56) is valid for the general effective action within the parameterisation  $\Gamma_k = \Gamma_{\text{diff}}[g, \bar{C}, C] + \Delta \Gamma[\bar{g}; h, \bar{C}, C]$  with diffeomorphism-invariant  $\Gamma_{\text{diff}}$ . The present approximation is the simplest case of such a splitting. In the full quantum case, the replacement  $\langle \hat{h}^a ; i \rangle \rightarrow h^a ; i$  is a mean field approximation,

$$\left. \langle \hat{h}^a ; i \rangle \right|_{\text{mean field}} = h^a ; i. \quad (57)$$

Using this approximation in (56), the first term on the left hand side vanishes and we arrive at

$$\Delta \Gamma_{k,i} + \Delta \Gamma_{k,a} h^a ; i = \frac{1}{2} G^{ab} \mathcal{R}_{ba,i} + \mathcal{R}_{ab} G^{bc} \frac{\delta}{\delta \bar{h}^c} h^a ; i. \quad (58)$$

Note that implicitly the mean field approximation is behind both, the Einstein-Hilbert approximation as well as the identity (54). The quantum deformation of diffeomorphism invariance encoded in  $\langle \hat{h}^a ; i \rangle - h^a ; i$  can be taken into account successively by the flow of  $\langle \hat{h}^a ; i \rangle$ , see [32]. This is postponed to future publications.

Eq. (58) can be used to compute the differences between the background parameters  $(\bar{\Lambda}, \bar{Z}_N)$  and the fluctuation parameters  $(\Lambda, Z_N)$  in the given Einstein-Hilbert approximation (40). We shall do this in an expansion about vanishing geodesic field  $h = 0$  as well as in an expansion of the  $\bar{g}$ -dependences of the regulator that induce the right hand side of (58). At  $h = 0$  we have

$$h^c ; a = -\delta^c_a, \quad h^d ; ca = 0,$$

$$h^d ; c(ab) = \frac{1}{6} (R_V^d{}_{acb} + R_V^d{}_{bca} + 2R_V^d{}_{c(ab)}), \quad (59)$$

the third derivative of  $h$  is proportional to the affine part of the curvature tensor  $R_V$  of Vilkovisky's connection. The  $R_V$ -terms would contribute to a further  $h$ -derivative of  $\Delta \Gamma_a[\bar{g}]$ . In the present work we drop them as sub-leading. Then, the last term in (58) vanishes and we conclude that

$$\Delta \Gamma_a[\bar{g}] = -\frac{1}{2} G^{cd} \mathcal{R}_{dc,a}[\bar{g}]. \quad (60)$$

This fixes the first two terms on the rhs of (45) which are computed with a further (covariant) derivative of  $\epsilon$  the first term on the rhs derives from  $\Delta \Gamma_2$ , (60) w.r.t.  $\sqrt{\bar{g}}$ . Now we take a  $h^b$ -derivative of (58) at fixed  $g$ . Evaluated at  $h = 0$  this reads

$$\Delta \Gamma_{ab}[\bar{g}] = -\Delta \Gamma_{b,a}[\bar{g}] - \frac{1}{2} \frac{\delta}{\delta h^b} (G^{cd} \mathcal{R}_{dc,a})[\bar{g}], \quad (61)$$

where the  $h^b$ -derivative of the flow term at fixed  $g$  only hits the cut-off terms and the  $\bar{g}$ -dependences of  $\Delta \Gamma^{(2)}$  in the propagator  $G$ , evaluated at  $h = 0$ . In combination this leads to a  $\bar{g}$ -derivative of  $-\Delta \Gamma_a[\bar{g}]$  at fixed regulator. In terms of the regulator-induced  $\bar{g}$ -dependences this is the leading term in the Nielsen-identity. Hence, within leading order we arrive at

$$\Delta \Gamma_{ab}[\bar{g}] = -\Delta \Gamma_{(b,a)}[\bar{g}] \equiv -\frac{1}{2} \Delta \Gamma_{b,a}[\bar{g}] - \frac{1}{2} \Delta \Gamma_{a,b}[\bar{g}]. \quad (62)$$

The results (62) and (60) allow us to compute  $\Delta \Gamma^{(2)}$  defined in (45),

$$\begin{aligned} \Delta \Gamma_{ab}^{(2)} &= -\frac{1}{2} (G^{cd} \mathcal{R}_{dc,(a,b)}) \\ &= -\frac{1}{2} (G^{cd} \mathcal{R}_{dc})_{,ab} + \frac{1}{2} (G^{cd}{}_{,(a} \mathcal{R}_{dc)})_{,b),} \end{aligned} \quad (63)$$

where as usual the parenthesis indicate symmetrization. For the flow of the propagator of the dynamical fields  $h$  on the right hand side of (24) we sum-up the  $t$ -derivative of (24) and  $\partial_t \Gamma_k[g]_{,ab}$ . The latter expression is the second derivative w.r.t.  $\bar{g}$  of the flow (22), evaluated at

$h = 0$ . Finally we need the covariant derivatives with the Vilkovisky connection of  $\Gamma_{\text{EH}}$  at vanishing fluctuation field  $h = 0$ . For the second derivative of  $\Delta\Gamma$  at  $h = 0$  this does not make a difference and we arrive at

$$\partial_t \Gamma_{k;ab}|_{h=0} = -\frac{1}{2}(\mathcal{R}_{dc}\partial_t G^{cd})_{;ab} + \frac{1}{2}\partial_t(\mathcal{R}_{dc}G^{cd})_{(;a);b}. \quad (64)$$

The first term on the right hand side is a total second derivative w.r.t.  $\bar{g}$ , and can be computed with heat kernel techniques analogously to the standard flow. In turn, the second term is not that easily accessible. However, it can be minimised by an appropriate regulator choice and will be discussed in the next Section. In summary the minimal consistent Einstein-Hilbert truncation (40) together with the flow of the fluctuation two-point function (64) allows us to compute the flow of all parameters,  $(g_N, \lambda)$  and  $(\bar{g}_N, \bar{\lambda})$ , in the given approximation.

## VI. PHASE DIAGRAM IN THE STANDARD BACKGROUND FIELD APPROXIMATION

We are now in the position to compute the flow of the couplings in the extended Einstein-Hilbert approximation put forward in Section IV. Given the close relation between the geometrical effective action and the background effective action in the Landau-DeWitt gauge, it is also worth discussing the similarities and the differences to the latter, see e.g. the reviews [6–8, 12] and the literature therein. Hence, for illustrative purposes and for the sake of comparison with results in the literature we first solve the geometrical flow equation in the background field approximation. This also allows us to disentangle the effects of this approximation from those arising from symmetry constraints. The background field approximation is implemented by identifying  $g_N \equiv \bar{g}_N$  and  $\lambda \equiv \bar{\lambda}$ , see [33]. This is achieved by taking  $\Delta\Gamma[\bar{g}, h] = 0$  in eq.(42) and evaluating the Einstein-Hilbert action  $\Gamma_{\text{EH}}[g; C, \bar{C}]$  at the background geometry  $g = \bar{g}$  and vanishing ghosts. Then the flow equation reduces to

$$\begin{aligned} \partial_t \Gamma_{\text{EH},k}[\bar{g}] &= -\text{Tr} \frac{1}{-\mathcal{Q}[\bar{g}] + \mathcal{R}_k^{gh}[\bar{g}]} \partial_t \mathcal{R}_k^{gh}[\bar{g}] \\ &+ \frac{1}{2} \text{Tr} \frac{1}{\nabla_\gamma^2 \Gamma_{\text{EH},k}[\bar{g}] + S_{\text{gf}}^{(2)}[\bar{g}] + \mathcal{R}_k^{\text{grav}}[\bar{g}]} \partial_t \mathcal{R}_k^{\text{grav}}[\bar{g}], \end{aligned} \quad (65)$$

where  $\mathcal{Q}$  is the ghost operator and the limit  $\alpha \rightarrow 0$  is implied. The traces in (65) only sum over momenta and internal indices. Following the common philosophy within the background field approach, we make the extra assumption that the gauge-fixing term has a  $Z$ -dependence, i.e:

$$S_{\text{gf}} = \frac{\bar{Z}_{N,k} \kappa^2}{4\alpha} \int d^d x \sqrt{\bar{g}} \bar{g}^{\tau\lambda} \mathcal{F}_\tau^{\rho'\sigma'}[\bar{g}] \hat{h}_{\rho'\sigma'} \mathcal{F}_\lambda^{\mu\nu}[\bar{g}] \hat{h}_{\mu\nu}. \quad (66)$$

This additional approximation (66) is resolved in the next Section VII. The rest of the present calculation proceeds

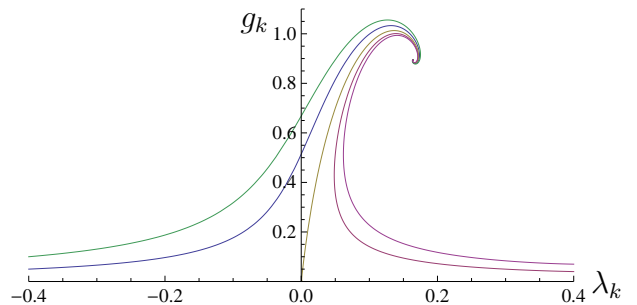


FIG. 2: Phase diagram in the background field approximation, (69), (70), with the UV fixed point  $(g_{N*}, \lambda_*) = (0.893, 0.164)$ .

by employing the standard York transverse-traceless decomposition detailed in Appendix A and choosing regulators whose tensor structure is adapted to this decomposition. The full set of regulators is listed in Appendix D. Here we explicitly provide the results for the optimised shape function, [46],

$$r(x) = (1-x)\theta(1-x). \quad (67)$$

With (67) the computations are much simplified. We use the York decomposition detailed in the Appendices A, B and the corresponding regulators in Appendix D with the optimised shape function (67). The relevant threshold functions for the optimised regulator are evaluated in Appendix F. The resulting flow equations read in four dimensions,  $d=4$ ,

$$\begin{aligned} \partial_t g_N - 2g_N &= \\ -\frac{g_N^2}{\pi} \frac{\frac{5}{3} + \frac{2}{3}(1-2\lambda) + \frac{25}{24}(1-2\lambda)^2}{(1-2\lambda)^2 - \frac{g_N}{2\pi} \left[ \frac{5}{9} + \frac{1}{3}(1-2\lambda) - \frac{5}{12}(1-2\lambda)^2 \right]}, \end{aligned} \quad (68)$$

and

$$\begin{aligned} \partial_t \lambda + 2\lambda &= \\ \eta_N \left( \lambda - \frac{g_N}{4\pi} \left( \frac{2}{3} + \frac{1}{1-2\lambda} \right) \right) - \frac{g_N}{4\pi} \left( 4 - \frac{6}{1-2\lambda} \right), \end{aligned} \quad (69)$$

with  $\eta_N$  defined in (49), (50). The two flow equations (69) and (70) define  $F_g$  and  $F_\lambda$  in (53a) and (53b) respectively in the standard background field approximation. The respective flow diagram is given in Fig. 2. The flow equations (69),(70) admit an attractive UV fixed point at

$$(g_{N*}, \lambda_*) = (0.893, 0.164), \quad (70)$$

and a repulsive Gaussian fixed point at the origin,  $(g_{N*}, \lambda_*) = (0, 0)$ , see also Fig. 2. We emphasize that (69) and (70) are completely independent of the gauge-fixing parameter  $\alpha$ . This is to be expected as the geometrical flow itself, by definition, does not depend on the gauge-fixing condition. This is in clear contradistinction

to  $\alpha$ -dependence observed in the usual background field approach, see [47, 48] and the reviews [6–8, 12].

Note also that the geometrical effective action at vanishing fluctuation field  $h = 0$  can be linked to the background effective action in the Landau-DeWitt gauge. In the present approach this matter is complicated due to the presence of the regulator and the approximation involved. We observe that in four dimensions,  $d = 4$ , the flow equations (69) and (70) indeed agree with the background flows with the optimised regulator [48]; however in dimensions  $d \neq 4$  the flows do not agree. The parameter  $a_2$  reads in the background field approach

$$a_2 = -\frac{d^3 - 4d^2 + 7d - 8}{2(d-1)}, \quad (71)$$

and differs from  $a_2$  in the geometrical approach, see (E4). This is not unexpected as the fluctuation fields in the present approach are non-polynomially related to the linear fluctuation fields in the standard background field approach.

## VII. DYNAMICAL FLOWS

In this section we set-up the full dynamical flow for the fluctuation field coefficients  $g_N$  and  $\lambda$ . The results apply to general background flows including the standard background approach. The latter can be obtained within the approximation discussed in the previous section, as well as in approximations going beyond (66). For the dynamical flow we have to evaluate (64). This can be done for general regulators with off-shell heat kernel techniques, see e.g. [49]. Here, however, we shall employ a specific choice of the regulator which removes the second term on the rhs, and also further facilitates the computations. To that end we choose the (partially) optimised regulator [9, 46] in (29) with the shape function in (67). This regulator renders all propagators constant for spectral values below the cut-off scale. Above the cut-off scale the regulator vanishes and hence  $\mathcal{R}\partial_t G_{;a} \equiv 0$ . Then (64) reduces to a total (covariant) derivative,

$$\partial_t \Gamma_{k;ab}|_{h=0} = -\frac{1}{2}(\mathcal{R}_{dc}\partial_t G^{cd})_{;ab}. \quad (72)$$

Eq. (72) can be computed with standard heat kernel techniques. Note that the optimisation in (29) serves a twofold purpose. First, it is the regulator choice partially adapted to the approximation specified in Section IV and hence maximises the physical content of the approximation. It only is a partial optimisation as the present choice does not fully resolve the issue of relative cut-off scales discussed in [9]. This entails that only the choice  $\theta \approx -1$  is optimised. Second, the choice (67) allows us to relate fluctuation flows and background flows with simple algebraic identities as will be shown below.

As a showcase for the full computation we shall evaluate the flow for  $\Lambda_k$  on a flat background  $\bar{g} = \eta$ . This

amounts to evaluating (72) on that background. However, as the rhs is explicitly a total second derivative it can be easily integrated. This leads us to

$$\partial_t (Z_{N,k} \Lambda_k) = -\frac{1}{4\kappa^2 \text{Vol}} \text{Tr} \mathcal{R}_k[\eta] \partial_t \frac{1}{\Gamma_k^{(2)}[\eta; 0] + \mathcal{R}_k[\eta]}, \quad (73)$$

where Vol stands for the volume factor  $\int d^4x \sqrt{\bar{g}}$ . It also occurs in the trace on the right hand side and hence drops out. With (73) we also get a simple relation between the flow of  $Z_{N,k} \Lambda_k$  and that of  $\bar{Z}_{N,k} \bar{\Lambda}_k$ ,

$$\begin{aligned} \partial_t (\bar{Z}_{N,k} \bar{\Lambda}_k) &= \partial_t (Z_{N,k} \Lambda_k) \\ &+ \frac{1}{4\kappa^2 \text{Vol}} \partial_t \left( \text{Tr} \mathcal{R}_k[\eta] \frac{1}{\Gamma_k^{(2)}[\eta; 0] + \mathcal{R}_k[\eta]} \right). \end{aligned} \quad (74)$$

For the regulator (67) the integrands in the traces in (73) and (74) agree up to prefactors. For the integrands in (73) we have a simple relation. For later purpose we already write it in its general form in the presence of a non-vanishing curvature,

$$\begin{aligned} \mathcal{R}_k^{\text{mode}} \partial_t \left( \frac{1}{k^2 Z} \frac{1}{1 + b_{\text{mode}} \rho + c_{\text{mode}} \lambda} \right) \\ = - \left( 2 - \eta_Z + \frac{c_{\text{mode}} \dot{\lambda} - 2b_{\text{mode}} \rho}{1 + b_{\text{mode}} \rho + c_{\text{mode}} \lambda} \right) \\ \times \mathcal{R}_k^{\text{mode}} \frac{1}{k^2 Z} \frac{1}{1 + b_{\text{mode}} \rho + c_{\text{mode}} \lambda}, \end{aligned} \quad (75)$$

The quadratic part of the action is detailed in the Appendices B,C and the regulator  $\mathcal{R}_k^{\text{mode}}$  of a given mode is a function of  $\Delta_{\bar{g}}$ , see Appendix D. This leads to the denominator in (75). We also have used the notation  $\dot{\lambda} = \partial_t \lambda$ , and have introduced the dimensionless curvature  $\rho$

$$\rho = R/k^2, \quad (76)$$

with  $\partial_t \rho = -2\rho$ . In (75) the coefficient  $c_{\text{mode}} = 0$ ,  $-d/(d-2)$  takes into account the  $\lambda$ -dependence of the different modes. In turn, the coefficients  $b_{\text{mode}}$  are more complicated. However, their specific value drops out for the computations done here. The different wave function renormalisations lead to anomalous dimensions

$$\eta_Z = -\partial_t \ln Z, \quad \dot{\lambda} = \partial_t \lambda. \quad (77)$$

Evidently the rhs of (75) is that of the integrand of the trace in (74) up to the prefactor in parenthesis. In (75) we have used the fact that the propagators are flat for  $\Delta_{\bar{g}} < k^2$ . The anomalous dimension  $\eta_Z$  is vanishing for ghosts in the present approximation due to  $Z_{\text{gh}} \equiv 1$ . Moreover, we have  $\eta_Z = \eta_N$  with  $Z = Z_N$  for the transversal graviton modes. For the gauge mode we have  $Z_\alpha = 1$ . It is only introduced for convenience and it flow vanishes due to diffeomorphism invariance. Then, with

(75) we compute (73) as

$$(\partial_t + (2 - \eta_N)) \lambda = 2(I_{\lambda,0} + I_{\lambda,\text{gh}}) \quad (78)$$

$$+ \left( 2 - \eta_N - \frac{\frac{d}{d-2} \dot{\lambda}}{1 - \frac{d}{d-2} \lambda} \right) I_{\lambda,-2},$$

with

$$I_{\lambda, \text{cmode}} = \frac{8\pi g_N}{k^d \text{Vol}} \text{Tr} \mathcal{R}_k^{\text{mode}}(\Delta_{\bar{g}}) \frac{1}{k^2 Z} \frac{1}{1 + c_{\text{mode}} \lambda}, \quad (79)$$

and similarly for  $I_{\lambda,\text{gh}}$ . The term  $2I_{\lambda,0}$  in (79) only comes from the gauge mode. The  $I$ 's defined in (79) also allow us to compute the second line in (74). This term depends on covariant momenta, the cut-off scale  $k$ , the normalised cosmological constant  $\lambda = \Lambda_k/k^2$ , and its canonical dimension is  $d$ . Therefore the trace in the second line in (74) leads to an explicit factor  $k^d$  multiplied by a function of  $\lambda$ . The  $t$ -derivative reproduces the term as well as a  $\dot{\lambda}\partial_\lambda$ -term. Hence we conclude that

$$\frac{8\pi g_N}{k^d \text{Vol}} \partial_t \left( \text{Tr} \mathcal{R}_k[\eta] \frac{1}{\Gamma_k^{(2)}[\eta; 0] + \mathcal{R}_k[\eta]} \right) \quad (80)$$

$$= d(I_{\lambda,0} + I_{\lambda,\text{gh}}) + \left( d + \frac{\frac{d}{d-2} \dot{\lambda}}{1 - \frac{d}{d-2} \lambda} \right) I_{\lambda,-2}.$$

Adding (80) to (78) gives the rhs of (74). Resolving this for the flow of  $\bar{\lambda}$  yields

$$\frac{g_N}{\bar{g}_N} (\partial_t + (2 - \bar{\eta}_N)) \bar{\lambda} = (d+2)(I_{\lambda,0} + I_{\lambda,\text{gh}})$$

$$+ (d+2 - \eta_N) I_{\lambda,-2}. \quad (81)$$

Eq. (81) is the standard background flow if we apply  $(g_N, \lambda) \rightarrow (\bar{g}_N, \bar{\lambda})$  on the right hand side. This allows us to determine the coefficient functions  $I_\lambda$  from the standard background field approximation to the flow. The coefficient functions  $I_\lambda$  are then inserted in the flow of  $\kappa^2 \Lambda_k$  in (78).

Note that even though (81) was derived in a flat background we have only used general properties and relations for the flow, and hence (78),(81) are valid for arbitrary backgrounds. Indeed we can even extend (81) to the full flow of the effective action in the Einstein-Hilbert approximation (40), (42) for general backgrounds with constant curvature  $R$ . In order to access the curvature term we first have to discuss (75) if we want to take derivatives w.r.t.  $R$ .

For the curvature term (80) has dimension  $d-2$  and hence we have  $d \rightarrow d-2$ . This leads to

$$-\frac{g_N}{\rho} \frac{8\pi g_N}{k^d \text{Vol}} \partial_t \left( \text{Tr} \mathcal{R}_k[\eta] \frac{1}{\Gamma_k^{(2)}[\eta; 0] + \mathcal{R}_k[\eta]} \right)_\rho = \quad (82)$$

$$(d-2)(I_{N,0} + I_{N,\text{gh}}) + (d-2 + \dot{\lambda}\partial_\lambda) I_{N,-2},$$

where the subscript  $\rho$  in the first line stands for the projection on the term linear in the curvature  $R$ , and  $\rho$  is the dimensionless curvature, see (76). Note that (82) is insensitive to the explicit occurrence of  $\rho$  in the propagator. Combining (82) with (75) we see, that the dimensional counting for the term linear in  $\rho$  gives a factor  $d-2$  for the modes without explicit curvature-dependence,  $b_{\text{mode}} = 0$ , and a factor  $d$  as for the cosmological constant for the terms with  $b_{\text{mode}} \neq 0$ . The dimensional prefactor does not depend on  $b_{\text{mode}}$ , whereas the coefficient  $I$  does. Hence we finally arrive at

$$\frac{8\pi g_N}{k^d \text{Vol}} \partial_t \Gamma_k[\bar{g}; 0] = (d+2)\mathcal{I}_\lambda - \eta_N I_{\lambda,-2}$$

$$- (d\mathcal{I}_N - \eta_N I_{N,-2}) \frac{\rho}{g_N} - 2\mathcal{I}_{N,1} \frac{\rho}{g_N}, \quad (83)$$

with

$$\mathcal{I}_\lambda = I_{\lambda,0} + I_{\lambda,\text{gh}} + I_{\lambda,-2},$$

$$\mathcal{I}_N = I_{N,0,0} + I_{N,\text{gh},0} + I_{\lambda,-2,0}$$

$$+ I_{N,0,1} + I_{N,\text{gh},1} + I_{\lambda,-2,1}. \quad (84)$$

In (84) the last subscript for the coefficients  $I_N$  with the values 0, 1 labels vanishing and non-vanishing  $b_{\text{mode}}$ , and  $\mathcal{I}_{N,0}, \mathcal{I}_{N,1}$  stand for the respective terms. Eq. (83) allows us to read-off the coefficients  $I_N$  and  $I_\lambda$  from the corresponding background field flows of  $\bar{g}_N$  and  $\bar{\lambda}$  respectively. With these coefficients we can derive the flow of  $g_N$  and  $\lambda$  similarly to (78). These flows can be summarised conveniently in

$$\frac{8\pi g_N}{k^d \text{Vol}} \partial_t \Gamma_{\text{EH}}[g; 0] \Big|_{\lambda, g_N} = 2\mathcal{I} - 2\mathcal{I}_{N,1} \frac{\rho}{g_N} \quad (85)$$

$$- (\eta_N + \dot{\lambda}\partial_\lambda) I_{-2},$$

where  $I_{-2} = I_{\lambda,-2} - I_{N,-2}\rho/g_N$  and  $\mathcal{I}_{N,1}$  stands for the second line in (84). The total coefficient  $\mathcal{I}$  is given by

$$\mathcal{I}(\lambda, g_N) = \mathcal{I}_\lambda(\lambda, g_N) - \mathcal{I}_N(\lambda, g_N) \frac{\rho}{g_N}. \quad (86)$$

The lhs of (85) is the flow of (39) with  $(\bar{Z}_N, \bar{\Lambda}) \rightarrow (Z_N, \Lambda)$ , and the rhs is projected on the respective terms proportional to  $r^0$  and  $r^1$ . Eq. (83) and (85) allow us to compute the flow of  $g_N$  and  $\lambda$  from a given background flow computed in the approximation (54), where  $\lambda \rightarrow \lambda$  on the right hand side of the background flow: the coefficient functions  $I$  are determined from (83) with  $\bar{Z}_N \rightarrow Z_N, \bar{\Lambda} \rightarrow \Lambda$  on the left-hand side and then identifying the terms proportional to  $\eta_N, \partial_t \lambda$  and the rest in the flows for  $g_N$  and  $\lambda$ . The coefficient functions  $I$  are then used in (85) which gives us the flow equations for the fluctuation parameters  $g_N, \lambda$  in (51). The physical observables  $\bar{g}_N, \bar{\lambda}$  derive from (83) with the results for

the fluctuation parameters  $g_N, \lambda$  inserted on the right-hand side. This gives us the flow equations (53).

Eq. (85) and the above relations complete our truncation: we use the flow of the effective action at vanishing fluctuation fields  $h = 0$  within the standard approximation  $\Gamma_{k,a} h^a{}_{;i} + \Gamma_{k,i} = 0$ . Furthermore we account for the full Nielsen identity with (85) and (83) being sensitive of the background field dependence in the regulator term. If we apply (85) and (83) for general regulators one has to bear in mind that this implies neglecting those terms in the Nielsen that are proportional to derivatives of the regulator  $\mathcal{R}_k(x)$  w.r.t the covariant momentum  $x$ . As has been argued, they are sub-leading, and indeed they can be minimised by using regulators that are sufficiently flat. In summary the geometrical approach provides us with a fully diffeomorphism-invariant flow for quantum gravity where we have also good qualitative control over the difference between fluctuation fields and background metric. The latter distinction is particularly important for the background independence of the results.

### VIII. PHASE DIAGRAM IN THE GEOMETRICAL BACKGROUND FIELD APPROXIMATION

The present diffeomorphism-invariant setting leads to a further simplification of the results in the previous Section VII. Due to the projection on transversal metric fluctuations the coefficient  $I_0$  vanishes identically,  $I_0 \equiv 0$ . With standard heat-kernel techniques and the York transverse-traceless decomposition we arrive after some algebra at the flows for the background Newton constant,

$$\frac{g_N}{\bar{g}_N} (\partial_t + (2 - d)) \bar{g}_N = \bar{F}_g^{(1)} - \eta_N \bar{F}_g^{(2)}, \quad (87)$$

and the background cosmological constant

$$\frac{g_N}{\bar{g}_N} (\partial_t + (2 - \bar{\eta}_N)) \bar{\lambda} = \bar{F}_\lambda^{(1)} - \eta_N \bar{F}_\lambda^{(2)}, \quad (88)$$

The  $\bar{F}^{(1)} g(\lambda, g)$  and  $\bar{F}^{(2)} g(\lambda, g)$  originate in terms in the flows proportional to  $\partial_t k^2 r$  and  $\partial_t Z_N$  respectively, and only depend on the dynamical couplings  $\lambda, g$ . They are given in terms of the coefficient functions  $I_\lambda$  and  $I_N$  which are detailed in Appendix E.

Note that we have chosen canonical dimensional factors  $d$  in the flow of the Newton constant  $\bar{g}_N$  in (87). Within the split in curvature-dependent and curvature-independent modes this implies

$$\begin{aligned} \bar{F}_g^{(1)} &= d\mathcal{I}_N + 2\mathcal{I}_{N,1}, \\ \bar{F}_g^{(2)} &= I_{N,-2}, \\ F_\lambda^{(1)} &= (d+2)\mathcal{I}_\lambda, \\ F_\lambda^{(2)} &= I_{\lambda,-2}, \end{aligned} \quad (89)$$

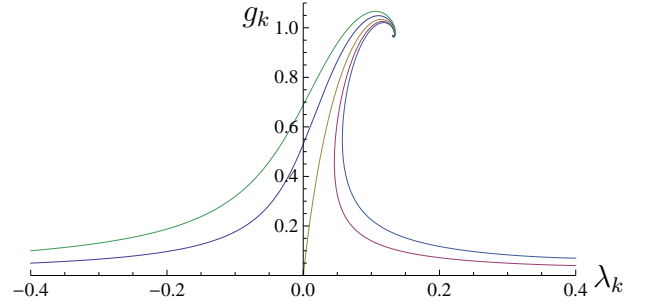


FIG. 3: Improved phase diagram for the background couplings, eqs.(90) and (91), with an UV fixed point  $(g_{N*}, \lambda_*) = (0.966, 0.132)$ .

with  $\mathcal{I}_N, \mathcal{I}_\lambda$  defined in (84) and the related coefficient functions  $F^{(1)}, F^{(2)}$  are given in Appendix F, (F5),(F7). The relations (89) are derived within the optimised regulator, (67), and the  $I$ 's in Appendix F satisfy the relations implied in (89). The system of flow equations (87), (88) constitutes one of the main results of the present work. It is a fully diffeomorphism-invariant flow for the pair of background couplings  $(\bar{g}_N, \bar{\lambda})$  beyond the background field approximation. There is no dependence on the gauge fixing parameter  $\alpha$  and the rhs in (87),(88) only depend on the dynamical couplings  $(g_N, \lambda)$ . Hence, the solution of (87),(88) requires that one solves the flows of the dynamical couplings first. Moreover, vanishing  $\beta$ -functions  $\partial_t \bar{g}_N = 0 = \partial_t \bar{\lambda}$  determine fixed point pairs  $(\hat{g}_N, \hat{\lambda})$ . Note, however, that the  $\beta$ -functions of the background couplings signal a fixed point only if the pair  $(\hat{g}_N, \hat{\lambda})$  is a fixed point of the dynamical flow.

Before we discuss the respective dynamical flows we first implement once more the background field approximation  $(g_N, \lambda) = (\bar{g}_N, \bar{\lambda})$ . Again we use the York decomposition detailed in the Appendices A, B and the corresponding regulators from Appendix D with the optimised shape function (67). The coefficient functions  $I_{\lambda,N}$  (with  $d = 4$ ) as well as the right hand sides of eqs.(51a) and (53a) can also be found in Appendix F. With the results of Appendix F we are finally led to the flow equations for the Newton constant and the cosmological constant,

$$\partial_t g_N - 2g_N = -\frac{g_N^2}{\pi} \frac{\frac{5}{3} + \frac{2}{3}(1-2\lambda) + \frac{25}{24}(1-2\lambda)^2}{(1-2\lambda)^2 - \frac{g_N}{2\pi} (\frac{5}{9} + \frac{1}{3}(1-2\lambda))}, \quad (90)$$

and

$$\partial_t \lambda + 2\lambda = \eta_N \left( \lambda - \frac{g_N}{4\pi} \frac{1}{1-2\lambda} \right) - \frac{g_N}{4\pi} \left( 4 - \frac{6}{1-2\lambda} \right), \quad (91)$$

with  $\eta_N$  defined in (49), (50). The respective flow diagram is given in Fig. 3. The flow equations (90),(91) admit an attractive UV fixed point at

$$(g_{N*}, \lambda_*) = (0.966, 0.132), \quad (92)$$

and a repulsive Gaussian fixed point at the origin,  $(g_{N*}, \lambda_*) = (0, 0)$ , see also Fig. 3.

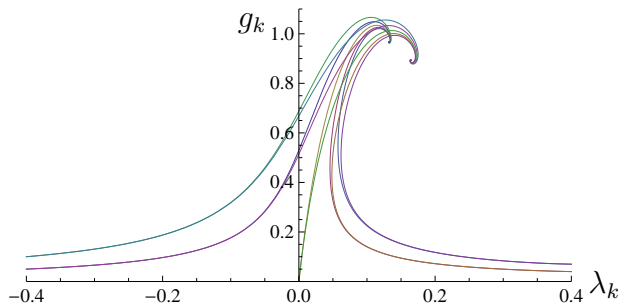


FIG. 4: Phase diagrams in the background field approximation from the flows (70), (92) in Section VI with FP (0.893, 0.164), and from the flows (90) and (91) with FP (0.966, 0.132).

Interestingly, the flows (87), (88) do not agree with those in Section VI, equations (69), (70). This leads to a different phase diagram, see Fig. 4, and different fixed point values, (70) and (92). We emphasise that the position of the fixed points are not physical observables and depend on the parameterisation of the theory. Indeed the differences depicted in Fig. 4 are small and are comparable to differences obtained by varying the regulators. The latter variation tests the stability of the approximation at hand as well as the reparameterisation independence. Moreover, the differences are fully explained by an additional approximation made in the standard background field approximation which is not present in the flows (87), (88). In turn, the flows in Section VI were constructed within the same approximation commonly used in the background field approach, see e.g. the reviews [6–8, 12] and literature therein. The only difference to the standard approximation in the background field approach in Section VI is the use of the covariant derivatives in the two point functions. As discussed in Section VI the two flows agreed in four dimensions. The difference to the present flows occurs in  $I_{\lambda, N}^{(2)}$ , the coefficients of  $\eta_N$  in the flow. It has but nothing to do with the difference between geometrical flow and background flow but relates to an additional approximation usually applied in the latter. For computational simplicity the wave function renormalisation  $Z_N$  has also been applied to all terms in the effective action, also to the gauge fixing term with  $Z_\alpha = Z_N$ . The latter term, however, does not run with  $Z_N$ . Indeed, any flow of the gauge fixing term only signals the breaking of diffeomorphism invariance. In the standard background field approach such a flow is induced by the cut-off term but does not agree with the flow of  $Z_N$ . In turn, in the present diffeomorphism-invariant setting  $Z_\alpha$  does not flow. This singles out the flows (87), (88) as the correct implementation of the background field approximation in the present setting. Due to the formal equivalence of both approaches in Landau-DeWitt gauge it is suggestive that one also should set  $Z_\alpha = 1$  in the standard background field flow. In conclusion the geometrical flow in the background field approximation agrees in four dimensions with the standard background

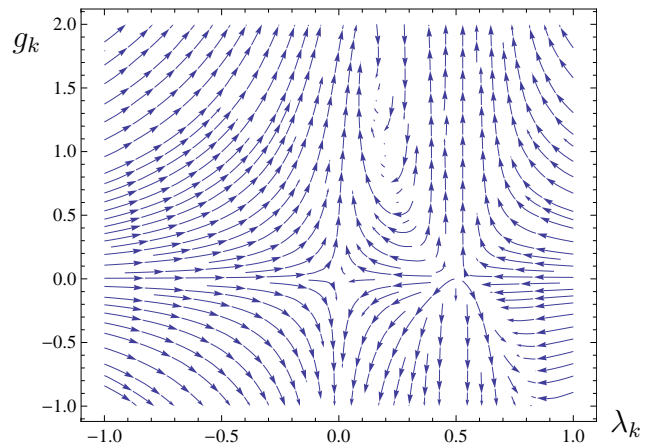


FIG. 5: Phase portrait of the dynamical flow in terms of the vector field  $(\partial_t g_N, \partial_t \lambda)$

field flow in the standard background field approximation within the Einstein-Hilbert truncation together with the above treatment of the gauge fixing term.

## IX. DYNAMICAL PHASE DIAGRAM & FIXED POINTS

Now we proceed to the full system including also the flow of fluctuation couplings  $(g_N, \lambda)$ . First we remark that for general regulators the flows (87), (88) do neither have the form (83), nor does the flow for  $(g_N, \lambda)$  have the form (85). This is only achieved for regulators leading to threshold functions  $\Phi$  and  $\tilde{\Phi}$ , see Appendix E, (E1), that satisfy

$$\Phi_{\frac{d-2}{2}}^1 / \tilde{\Phi}_{\frac{d-2}{2}}^1 = \frac{d}{2}, \quad \Phi_{\frac{d}{2}}^2 / \tilde{\Phi}_{\frac{d}{2}}^2 = \frac{d+2}{2}, \quad (93)$$

Eq. (93) holds for the optimised regulator, see (F3). Note that the latter was used to derive (83), (85) in the first place. Evidently, (93) holds for a larger class of regulators as it comprises only two integral constraints on a given regulator. However, if one improves the current approximation, further constraints arise, leading to (F2) for  $n = d/2$  and  $(d-2)/2$ . This uniquely singles-out the optimised regulator. For general regulators one might compute all the necessary coefficient functions. However, it is more convenient to use the approximation (93) on the basis of explicitly computing  $F^{(2)}$ . Within this approximation it is easily possible to map the known background results in the literature to the full flow where one distinguishes between dynamical fluctuation fields and background fields.

We continue with our analysis of the optimised flow. The flow equations of the dynamical fluctuation couplings  $(g_N, \lambda)$  follow from (85) as

$$(\partial_t + (2-d))g_N = 2\mathcal{I}_N + 2\mathcal{I}_{N,1} - \left(\eta_N + \dot{\lambda}\partial_\lambda\right)I_{N,-2}, \quad (94)$$

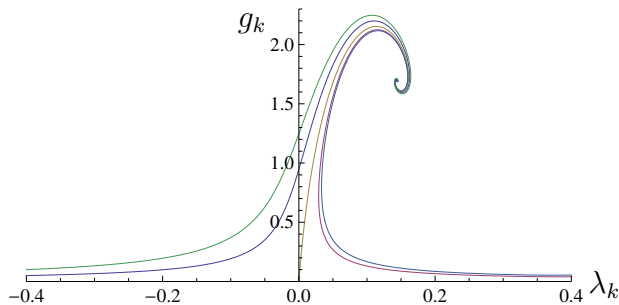


FIG. 6: Phase diagram for the dynamical couplings, (96) and (97), with an UV fixed point  $(g_{N*}, \lambda_*) = (1.692, 0.144)$ , and the repulsive perturbative fixed point  $\text{FP}_{\text{rep}} = (0, 0)$ .

with  $\mathcal{I}_N$  defined in (84) and

$$(\partial_t + (2 - \eta_N))\lambda = 2\mathcal{I}_\lambda - (\eta_N + \lambda\partial_\lambda)I_{\lambda,-2}, \quad (95)$$

and (93) holds. The coefficient functions  $I_{\lambda,N}$  (with  $d = 4$ ) have been already used for the flows in the background couplings, (90), (91). Together with the right hand sides of (51a) and (53a) they can be found in Appendix F. With the results of Appendix F we arrive at the flow equations for the dynamical couplings  $g_N, \lambda$ ,

$$\begin{aligned} \partial_t g_N &= 2g_N - \frac{g_N^2}{\pi} \frac{\frac{5}{9} + \frac{1}{3}(1-2\lambda) + \frac{5}{9} \frac{25}{24}(1-2\lambda)^2}{(1-2\lambda)^2 - \frac{g_N}{2\pi} (\frac{5}{9} + \frac{1}{3}(1-2\lambda))} \\ &+ \frac{2\partial_t \lambda}{1-2\lambda} \frac{g_N^2}{2\pi} \frac{\frac{10}{9} + \frac{1}{3}(1-2\lambda)}{(1-2\lambda)^2 - \frac{g_N}{2\pi} (\frac{5}{9} + \frac{1}{3}(1-2\lambda))}, \quad (96) \end{aligned}$$

and

$$\partial_t \lambda = \frac{-(2 - \eta_N)\lambda + (2 - \eta_N) \frac{g_N}{4\pi} \frac{1}{1-2\lambda} - \frac{g_N}{3\pi}}{1 + \frac{g_N}{2\pi} \frac{1}{(1-2\lambda)^2}}, \quad (97)$$

with  $\eta_N$  defined in (49), (50). The flow equations (96) and (97) describe the phase diagram of quantum gravity in the extended Einstein-Hilbert truncation in terms of the dynamical couplings  $g_N, \lambda$ . The vector fields of the corresponding  $\beta$ -functions are depicted in Fig. 5. In comparison to the standard background flows (69), (70) and the geometrical background flows (90), (91) they contain a further resummation. The related terms are given with the second line in (96) and the non-trivial denominator in (97). They are related to scale derivatives  $\partial_t \lambda$  and can be understood in terms of standard 2PI and hard thermal loop resummations of the self energy or mass in quantum field theory, see [50] for the FRG implementation. This new, additional resummation removes the infrared singularity in the flows at  $\lambda = 1/2$  present in the background field flows but introduces new repulsive singularities in the flow of the Newton constant  $g_N$ . This is very reminiscent of the screening of the infrared singularity in thermal theories and is discussed in Section IX B.

The phase portrait in Fig. 5 shows an attractive UV fixed point as well as a repulsive Gaussian fixed point

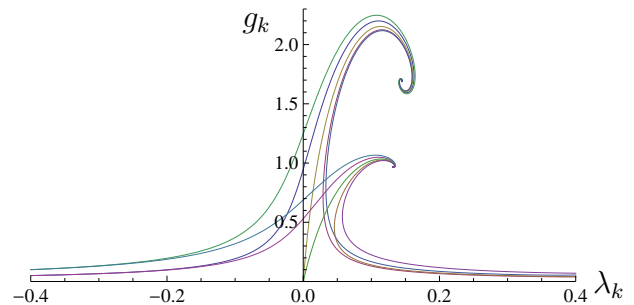


FIG. 7: Phase diagrams in the background field approximation from the flows (90) and (91) with the UV fixed point  $(0.966, 0.132)$ , and from the dynamical flows (96) and (97) with the UV fixed point  $(1.692, 0.144)$ .

at the origin in analogy to the background field approximations. It also shows an attractive IR fixed point at  $g_N = 0$  and  $\lambda = 1/2$  as well as repulsive lines emanating from the IR fixed point.

### A. UV fixed point

The second line in (96) drops out at a fixed point. The flow equations (96),(97) admit an attractive UV fixed point at

$$\text{FP}_{\text{UV}} = (g_{N*}, \lambda_*) = (1.692, 0.144), \quad (98)$$

and a repulsive Gaussian fixed point at the origin,  $\text{FP}_{\text{rep}} = (g_{N*}, \lambda_*) = (0, 0)$ , see also Fig. 6. The flow diagram and the fixed point differs from that in the background field approximation depicted in Fig. 3. A comparison of the respective phase diagrams is depicted in Fig. 7. The difference of the two phase diagrams in Fig. 7 is qualitatively different from that between the two background field approximations discussed before. It is not comparable to differences obtained by varying the regulator. This is best seen by studying the product of Newton constant and cosmological constant which is significantly reduced for the dynamical flow in comparison to the background field approximation, see Table I. We have also included a comparison to fixed points derived within the bimetric flows studied in [40]. While the positions of the fixed points for the dynamical and bimetric flows are quite different, the invariant product  $g_{N*}\lambda_*$  only deviated by a few percent.

TABLE I: Fixed Points

Type of flow	$g_{N*}$	$\lambda_*$	$g_{N*} \times \lambda_*$
Background	0.893	0.164	0.146
Improved background	0.966	0.132	0.128
Dynamical	1.692	0.144	0.244
Bimetric	1.055	0.222	0.234

TABLE II: Stability matrices

Flows	Stability matrix	Eigenvalues
Background	$\begin{pmatrix} -2.46 & -10.52 \\ 0.71 & -1.61 \end{pmatrix}$	$-2.03 + 2.69i$ $-2.03 - 2.69i$
Improved backgr.	$\begin{pmatrix} -2.59 & -9.99 \\ 0.47 & -2.01 \end{pmatrix}$	$-2.30 - 2.16i$ $-2.30 - 2.16i$
Dynamical	$\begin{pmatrix} -1.94 & -27.9 \\ 0.26 & -0.74 \end{pmatrix}$	$-1.34 + 2.61i$ $-1.34 - 2.61i$

The stability matrices are displayed in Table II, the bending around the fixed point, which is introduced by the imaginary part of the eigenvalues, is reduced from the standard background field approximation to the improved one. For the dynamical flows, the bending is stronger which comes from the  $\partial_t \lambda$ -terms in the flows. Without these terms the bending is even reduced further in comparison to the improved background flows. This leads to a far smaller bending of the phase diagram about the fixed points, see Fig. 7.

### B. IR fixed points & phase diagram

Finally, we would like to discuss the infrared behaviour of the full dynamical flows (96),(97). A similar investigation was first done in [51] within the background field approach. The resummation due to the  $\partial_t \lambda$ -terms screens the singularity in the propagators at  $1 - 2\lambda = 0$  similarly to the screening of thermal infrared singularities via thermal resummations. However, the resummations related to  $\eta_N$  on the right hand side of the flow lead to singular lines in the flow diagram, where both flows,  $\partial_t g_N$  and  $\partial_t \lambda$ , exhibit poles at

$$g_N^\pm = \frac{1}{5}\pi \left[ -(1 - 2\lambda) + 22\lambda(1 - 2\lambda) \pm \sqrt{\lambda(1 - 2\lambda)^2(179 - 676\lambda + 236\lambda^2)} \right]. \quad (99)$$

The singular lines terminate at  $(g_N, \lambda) = (1.414, 0.295)$ , and  $(g_N, \lambda) = (0, 1/2)$ . Such singular lines are as well present in the background field flows as they also include resummations related to  $\eta_N$ . Here we concentrate on positive cosmological constant where the background flows exhibit singular lines that terminates at  $\lambda = 4/3$  (improved background flow) or at  $\lambda = 1/30(9 \pm 4\sqrt{21})$  (standard background flow) and extend to  $\lambda = 0$ . The singular lines are displayed in Fig. 8.

All flows go through the point  $(\lambda, g_N) = (1/2, 0)$ , for the background flows, however, the  $\lambda$  axis is tangential to the singular lines at  $(1/2, 0)$ . For the dynamical flow the area under the singular line is restricted by  $g_-$  in (99). All flows in this area hit the singular line at some point: let us assume that there are flows that go to  $(1/2, 0)$  without hitting the singular line. Then, in the vicinity of

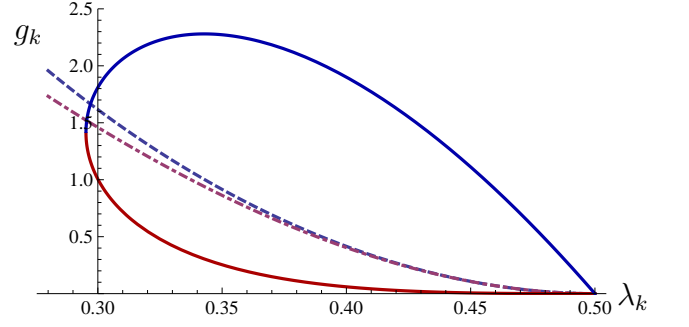


FIG. 8: Singular lines for the infrared-directed flow  $(-\partial_t g_N, -\partial_t \lambda)$ . The dashed, dotted and full lines are the singular lines for the standard background, the improved background and the dynamical flow respectively.

$(1/2, 0)$  we expand  $g_N^-$  about  $\lambda = 1/2$ , leading to

$$g_N^- = \frac{9}{5}\pi(1 - 2\lambda)^3 + O[(1 - 2\lambda)^4]. \quad (100)$$

This entails that the dynamical flows, (96) and (97), reduce to

$$\partial_t g_N = 2g_N(1 + \partial_t \lambda), \quad \partial_t \lambda = -(2 - \eta_N)\lambda, \quad (101)$$

which implies that  $\partial_t g_N = -4g_N/(1 - 2\lambda) < 0$  in leading order. Hence, with (101) we conclude that all trajectories in the vicinity of  $\lambda = 1/2$  hit the singular lines. On the lower singular line given by  $g_N^-$  the infrared-directed flows diverge but point towards the singular line. Hence this line is infrared stable. Moreover, there is a finite net flow on this singular line which comes from the sum of the (singular) flows taken at both sides of the singular line: we define unit infrared-directed tangential vectors  $\hat{e}(\lambda, g_N)$  to given trajectories with

$$\hat{e}(\lambda, g_N) = \frac{\vec{\beta}}{\|\vec{\beta}\|}, \quad \vec{\beta}(\lambda, g_N) = -(\partial_t \lambda, \partial_t g_N), \quad (102)$$

and the tangential vector on the singular line as a function of  $\lambda$  is given by

$$\hat{e}_\pm(\lambda) = \frac{1}{\sqrt{1 + (\partial_\lambda g_N^\pm)^2}}(1, \partial_\lambda g_N^\pm). \quad (103)$$

The  $e_\pm$  point towards  $(1/2, 0)$  along the respective singular line given by  $g_N^\pm$ . The corresponding orthogonal boundary vectors  $\hat{e}_\pm^\perp$ , directed away from the region bounded by the singular line, are given by

$$\hat{e}_\pm^\perp(\lambda) = \pm \frac{1}{\sqrt{1 + (\partial_\lambda g_N^\pm)^2}}(-\partial_\lambda g_N^\pm, 1). \quad (104)$$

The above definitions allow us to define the finite net flow vector  $\vec{\beta}_{\text{net}}$  on the singular line and the corresponding

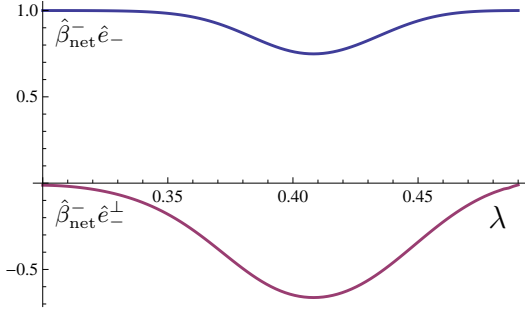


FIG. 9: Coefficients of the unit net flow on the singular line given by  $g_N^-$ , (99), directed towards  $(1/2, 0)$ .

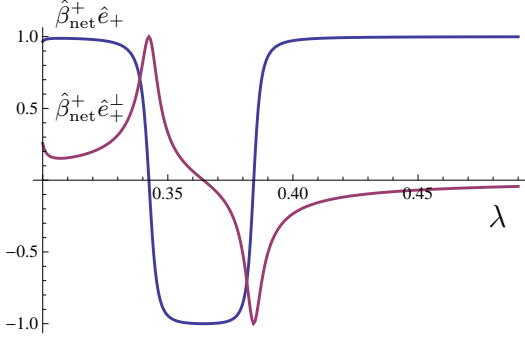


FIG. 10: Coefficients of the unit net flow on the singular line given by  $g_N^+$ , (99), directed towards  $(1/2, 0)$ .

unit flow vector  $\hat{\beta}_{net}$  are given by

$$\begin{aligned} \vec{\beta}_{net}^\pm &= \lim_{\epsilon \rightarrow 0} \frac{1}{2} \left[ \vec{\beta}((\lambda, g_N^\pm) + \epsilon \hat{e}_\pm(\lambda)) \right. \\ &\quad \left. + \vec{\beta}((\lambda, g_N^\pm) - \epsilon \hat{e}_\pm(\lambda)) \right], \\ \hat{\beta}_{net} &= \frac{\vec{\beta}_{net}}{\|\vec{\beta}_{net}\|}. \end{aligned} \quad (105)$$

In case of the infrared stable part of the singular line there is a flow along the singular line with the strength  $|\vec{\beta}_{net} \cdot \hat{e}|$ . The direction is given by the sign of  $\cos \theta = \hat{\beta}_{net} \cdot \hat{e}$  where  $\theta$  is the angle between  $\vec{\beta}_{net}$  and  $\hat{e}$ . This is plotted in Figs. 9, 10 and 11. In these figures we also plot  $\cos \theta^\perp = \hat{\beta}_{net} \cdot \hat{e}^\perp$  which encodes the information, whether the net flow is directed into the region bounded by the singular line or away from it. The full phase portrait is depicted in Fig. 12 and Fig. 13.

Most importantly, the projected net flow  $\hat{\beta}_{net}^- \cdot \hat{e}_-$  on  $g_N^-$  is directed towards  $(1/2, 0)$ . Hence the lower singular line is fully infrared stable, see Fig.9. The infrared attractive point  $(1/2, 0)$  is reached after a finite flow time at the cut-off scale  $k_0$ . For  $k < k_0$  the flows are trivial,

$$\partial_t g_N = 0, \quad \partial_t \lambda = -2\lambda \quad \rightarrow \quad g_N = 0, \quad \lambda = \frac{k_0^2}{2k^2}. \quad (106)$$

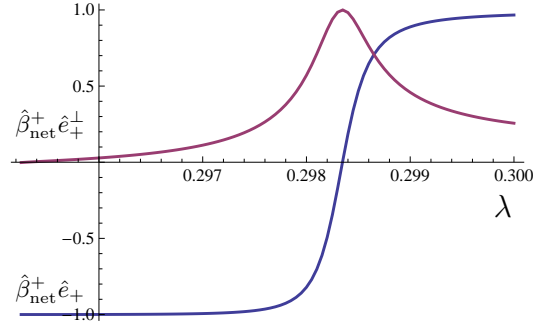


FIG. 11: Coefficients of the unit net flow on the singular line given by  $g_N^+$ , (99), directed towards  $(1/2, 0)$  in the vicinity of the turning point.

Eq. (106) reflects a trivial fixed point of a free massive theory. Note that this interpretation should be taken with caution due to the singularities. This concerns in particular the quantitative results, such as  $g_N \lambda = 0$  in the infrared. In summary we are led to the UV-IR stable region Ia with the UV-attractive fixed point  $FP_{UV} = (1.692, 0.144)$  and the IR-attractive fixed point  $FP_{IR,1} = (0, 1/2)$ , see Fig. 12. In turn, at the turning point of the singular line,  $g_+ = g_-$  with vertical tangential vector,

$$\lambda = \frac{(169 - 60\sqrt{5})}{118}, \quad g_N^+ = g_N^- = \frac{120\pi(301\sqrt{5} - 660)}{3481}, \quad (107)$$

the sign of  $\cos \theta^\perp$  turns positive and the net flow is directed away from the singular line. As this is also true for the full  $\beta$  functions, the singular line gets infrared unstable (and ultraviolet stable), see Fig. 11. In any case, no flow from the UV fixed point can reach this part of the singular line. This defines a separatrix from the UV fixed point to the turning point  $(0.295, 1.414)$  of the singular line with  $g_+ = g_-$ , see (107). Flows below this separatrix are driven towards the attractive infrared fixed point  $(1/2, 0)$ , flows above the separatrix are driven towards the attractive infrared fixed point  $(-\infty, 0)$ . In summary this leads the UV-IR stable region I with the UV attractive fixed point  $FP_{UV} = (1.692, 0.144)$ , the repulsive fixed point  $FP_{rep} = (0, 0)$  and the two IR attractive fixed points  $FP_{IR,1} = (1/2, 0)$  and  $FP_{IR,2} = (-\infty, 0)$ . Similar results have been obtained in the standard background field approach in [51].

The region II in Fig. 13 can be accessed from the infrared fixed point  $FP_{IR,2}$ . UV flows in this region hit the singular line between  $0.295 < \lambda < 0.327$ , depicted by the upper light blue and left dark blue dots in Fig. 12. We remark that this part of  $g_N^+$  is ultraviolet attractive and UV flows are driven towards  $\lambda = 0.298$  on the singular line. Accordingly there is a potential further UV attractive fixed point at  $FP_{UV,2} = (0.298, 1.738)$ , depicted with a violet dot in Fig. 12. This singles out the second IR-UV attractive region II. Note that this may very likely be an artefact of the approximation. Still it is worth further consideration.

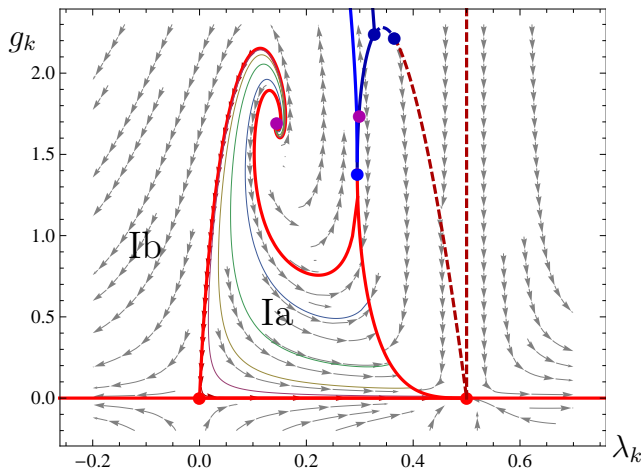


FIG. 12: Full phase diagram for the dynamical couplings including the repulsive perturbative fixed point  $FP_{\text{rep}} = (0, 0)$  and  $FP_{\text{IR},1} = (1/2, 0)$ . The red boundary lines show the separatrices.

The regions III and IV cannot be accessed from the UV fixed points nor do flows in the regions III and IV reach the infrared fixed points  $FP_{\text{IR},1}$  or  $FP_{\text{IR},2}$ . Infrared flows in this region are driven towards  $(\infty, 0)$  or  $(\infty, \infty)$ .

The same analysis can be made for the standard background and improved background approximation. We only mention that there exists regions similar to region Ia, and flows are directed towards the endpoint  $(1/2, 0)$  for  $\lambda > 0.4635$  (improved background) and for  $\lambda > 0.4637$  (standard background). Interestingly for both flows the scalar product  $\vec{\beta}_{\text{net}} \cdot \hat{e}_-$  is also positive for  $\lambda < 0.341$  (improved background) and for  $\lambda > 0.335$  (standard background). This leads to a further infrared stable point at  $(\lambda, g_N) = (0.341, 0.966)$  and  $(\lambda, g_N) = (0.335, 1.108)$  respectively.

In summary all flows exhibit a region which is ultraviolet and infrared stable. This is depicted for the dynamical flows in Figs. 12,13. At the IR fixed point  $FP_{\text{IR},2} = (1/2, 0)$  the product  $g_N \lambda = 0$ . Hence,  $\lambda$  vanishes in terms of  $g_N$  in the infrared. Note however, that  $\lambda$  is simply a parameter in the propagator of the fluctuation field  $h$  and its interpretation as the cosmological constant is not straightforward.

### C. Matrix elements & observables

It is left to determine physics observables such as the strength of the gravitational interaction measure in experiments. Here we only present the flow equations for the physical Newton coupling and cosmological constant and discuss the consistency of the results with the analysis made so far. Note first, that the dynamical couplings  $g_N, \lambda$  are only indirectly related to physics observables. This is a property the geometrical approach shares with the standard background field approach to quantum field

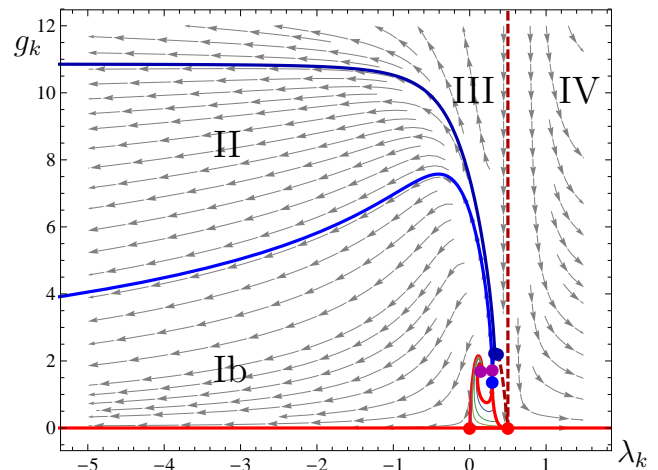


FIG. 13: Full phase diagram for the dynamical couplings including the repulsive perturbative fixed point  $FP_{\text{IR},0} = (0, 0)$ , and the attractive IR fixed points  $FP_{\text{IR},1} = (1/2, 0)$  and  $FP_{\text{IR},2} = (-\infty, 0)$ .

theory. However, we have also seen, that the background couplings are sensitive to the regulator. This holds in particular in the scaling regions: the regulators have been chosen such that they show the same (singular) scaling as the corresponding two-point functions  $\Gamma^{(2)}$ . Such regulators are called RG-adapted, [9, 41], or spectrally adjusted, [52]. The effective action satisfies the RG and scaling equations of the underlying full theory at vanishing cut-off, see [9, 41]. This property facilitates the access to scaling regions and relates to a partial optimisation of the flow, [9], but complicates the extraction of the physical part of the background field correlation functions. It has been shown in the standard background field approach that the regulator-induced terms can even change the sign of the  $\beta$ -functions, see [43], in the context of gravity this has been discussed in [28].

In the geometrical approach it is the Nielsen identity (55) that controls the difference between background field dependence and fluctuation field dependence, the right hand side being the term stemming from the regulator, see [9, 32]. Hence, at vanishing fluctuation field  $h = 0$  the physical background field dependence is comprised in the standard Nielsen identity

$$\Gamma_{k,i}|_{\text{phys}}[h=0] = -\Gamma_{k,a}\langle \hat{h}^a{}_{;i} \rangle[h=0]. \quad (108)$$

Eq. (108) entails that at  $h = 0$  we can identify the  $h$ -derivatives with the  $\bar{g}$ -derivatives up to sub-leading order. In other words, the physical part of the background couplings,  $\bar{g}_{N,\text{phys}}, \bar{\lambda}_{\text{phys}}$  have  $\beta$ -functions similar to that of the dynamical couplings. Note that this argument fully works the infrared where the regulator tends to zero and the sub-leading terms are small. It has to be taken with caution for large regulators. Thus we shall only discuss the infrared region with  $\lambda > 1/2$ : neglecting the sub-leading terms we arrive at the flow for the physical part

of the background Newton constant,

$$\frac{1}{\bar{g}_{N,\text{phys}}} (\partial_t + (2 - d)) \bar{g}_{N,\text{phys}} = \frac{1}{g_N} F_g(g_N, \lambda), \quad (109)$$

and the physical part of the cosmological constant  $\bar{\lambda}$

$$\frac{1}{\bar{g}_{N,\text{phys}}} (\partial_t + (2 - \bar{\eta}_N)) \bar{\lambda}_{\text{phys}} = \frac{1}{g_N} F_\lambda(g_N, \lambda). \quad (110)$$

For the optimised flows the right hand sides  $F_g$  and  $F_\lambda$  are given in (F9) and (F10) respectively. If identifying the physical part of the background couplings with the dynamical ones,  $(\bar{g}_{N,\text{phys}}, \bar{\lambda}_{\text{phys}}) = (g_N, \lambda)$ , we are led to the full flow of the dynamical couplings, (96), (97). We also remark that with (109),(110) we can derive finite net flows of  $g_{N,\text{phys}}$ ,  $\lambda_{\text{phys}}$  on the singular lines. There, however, the sub-leading terms might not be negligible.

Here we only consider  $\lambda > 1/2$  with  $k > k_0$ . Then the flows (109),(110) have to be evaluated for  $g_N = 0$ , to wit

$$\begin{aligned} \partial_t \bar{g}_{N,\text{phys}} &= 2\bar{g}_{N,\text{phys}}, \\ \partial_t \bar{\lambda}_{\text{phys}} &= -2\bar{\lambda}_{\text{phys}} + \frac{\bar{g}_{N,\text{phys}}}{6\pi} \frac{1 + 8\lambda(1 - \lambda)}{(1 - 2\lambda)^2}. \end{aligned} \quad (111)$$

Eq. (111) implies that  $\bar{g}_{N,\text{phys}} \propto k^2$  for  $k \rightarrow 0$ . We also have  $\lambda \propto 1/k^2$  due to (106) and we arrive at

$$\partial_t \bar{g}_{N,\text{phys}} = 2\bar{g}_{N,\text{phys}}, \quad \lambda_{\text{phys}} = -2\bar{\lambda}_{\text{phys}}, \quad (112)$$

for  $k \rightarrow 0$ . Eq. (112) simply provides the dimensional running of Newton constant and cosmological constant. It implies a finite product  $g_{N,\text{phys}} \lambda_{\text{phys}}$ , the value of which depends on the initial conditions. We conclude that the phase diagram of quantum gravity in the current approximation shows UV-IR stability. In the infrared region we are driven towards classical Einstein gravity.

## X. SUMMARY AND OUTLOOK

We close with a brief survey of our results, more detailed discussions can be found in the respective sections. In the present work we have established a fully diffeomorphism-invariant flow for gravity. This flow has also been shown to be gauge independent in [32]. In Section VI we have shown that the flow agrees in the linear approximation with the standard background approximation for the background field flow in Landau-DeWitt gauge. The latter approximation also implies an artificial scale-dependence (on the wave function renormalisation  $Z_N$ ) of the longitudinal degrees of freedom. Note however, that the scaling of the longitudinal (gauge) degrees of freedom indeed vanishes identically in the geometrical approach, whereas it only reflects the deformation of diffeomorphism invariance in the standard background field approach. We are hence lead to the same flow diagrams and fixed points, and the UV fixed point is given by in

Table I. Beyond the linear approximation the two flows differ in dimensions others than four but still agree for four dimensions. We have also introduced an improved background field approximation where care is taken of the fact that the longitudinal gauge direction do not flow. The related fixed point does not differ significantly from the standard background field result, see Table I.

Furthermore, we have introduced the difference between the background metric and the fluctuation metric. This difference has been evaluated by means of the Nielsen identity derived in [32], for the background approach analogue see [28, 41–43]. While the fixed point values of the couplings  $(g_N, \lambda)$  have no direct physical meaning, their dimensionless product  $g_N \lambda = G_N \Lambda$  differs considerably from that in the background approximation. It agrees very well with that in the bimetric background field approach, e.g. [40, 53], see Table I.

We have also discussed the infrared behaviour of quantum gravity in the present approach. Within the present approximation the flows run into a singularity at  $2\lambda = 1$  which signals a pole in the propagator. We emphasise that  $\lambda = \Lambda/k^2$  is the cosmological constant measured in the cut-off scale. The physical information is stored in  $g_N \lambda$ , that is, one measures the cosmological constant in units of the Newton coupling. There are further singularities in the  $\beta$ -functions which are related to the (incomplete) resummations put forward in the present paper. Still one can define finite net flows on these singular lines, and hence discuss the resulting phase diagram. A detailed analysis of the phase diagram reveals a very rich and interesting structure which is discussed in detail in Section IX B. Note that the respective results have to be taken with caution. Taking this into account we find an infrared stable fixed point at  $\text{FP}_{\text{IR}} = (g_{N*}, \lambda_{*})_{\text{IR}} = (0, 1/2)$  for the dynamical couplings. Similarly to the standard background field approach these dynamical parameters have to be mapped to the physical couplings. This has been done in the last Section IX C where it has been shown that in the infrared the theory tends towards classical Einstein gravity.

In summary the present analysis provides the first results within the fully diffeomorphism-invariant framework introduced in [31, 32]. Additionally it resolves the difference between fluctuating field and background metric via the Nielsen identity [32]. The results of the present work further solidify the asymptotic safety scenario for quantum gravity. A more detailed qualitative analysis also reveals a rich phase structure of quantum gravity including attractive infrared fixed points. In the infrared the theory tends towards classical Einstein gravity. The quantitative understanding of the full phase diagram of quantum gravity has to be furthered in more elaborated approximations.

*Acknowledgements* – We thank N. Christiansen, S. Folkerts, D. F. Litim, M. Reuter, A. Rodigast and F. Saueressig for discussions. JMP thanks D. F. Litim for repeated discussions on the infrared behaviour of gravity and sharing the unpublished results of [51].

### Appendix A: York decomposition

In the present work we use the York transverse-traceless decomposition, first introduced in Section III below (28). For more details in the context of FRG-flows see e.g. the reviews [6–8] and literature therein, as well as [33]. The York decomposition amounts to the decomposition of  $h$ ,

$$h_{\mu\nu} = h_{\mu\nu}^T + h_{\mu\nu}^{LT} + h_{\mu\nu}^{LL} + h_{\mu\nu}^{Tr}. \quad (\text{A1})$$

Here  $h_{\mu\nu}^{Tr}$  is the trace part of  $h_{\mu\nu}$  and the first three terms  $h_{\mu\nu}^T + h_{\mu\nu}^{LT} + h_{\mu\nu}^{LL}$  comprise its traceless component. We have the following well-known identities

$$\begin{aligned} h_{\mu\nu}^T &= \bar{\nabla}_\mu \xi_\nu + \bar{\nabla}_\nu \xi_\mu, \\ h_{\mu\nu}^{LT} &= (\bar{\nabla}_\mu \bar{\nabla}_\nu - \frac{1}{d} \bar{g}_{\mu\nu} \bar{\Delta}) \sigma, \\ h_{\mu\nu}^{LL} &= \frac{1}{d} \bar{g}_{\mu\nu} \varphi, \end{aligned} \quad (\text{A2})$$

where  $\xi_\mu$  is a transverse vector field and  $\sigma$  and  $\varphi$  are scalar fields. The tensor fields, appearing in this decomposition, obey the following relations,

$$\bar{g}^{\mu\nu} h_{\mu\nu}^T = 0, \quad \bar{\nabla}^\mu h_{\mu\nu}^T = 0, \quad \bar{\nabla}^\mu \xi_\mu = 0, \quad \varphi = \bar{g}^{\mu\nu} h_{\mu\nu}. \quad (\text{A3})$$

The scalar field can be further split into two parts  $\varphi = \varphi_0 + \varphi_1$  with  $\varphi_0$  being orthogonal to  $\varphi_1$  and  $\hat{\sigma}$ , for the details we refer the reader to the literature.

Additionally we decompose the ghost as follows

$$C^\mu = C^{T,\mu} + \bar{\nabla}^\mu \rho, \quad \bar{C}_\mu = \bar{C}_\mu^T + \bar{\nabla}_\mu \bar{\rho}, \quad (\text{A4})$$

where  $\bar{C}_\mu^T$  and  $C^{T,\mu}$  are the transverse components of  $\bar{C}_\mu$  and  $C^\mu$ , i.e.  $\bar{\nabla}^\mu \bar{C}_\mu^T = 0$  and  $\bar{\nabla}_\mu C^{T,\mu} = 0$ , and  $\bar{\rho}, \rho$  are scalar fields.

### Appendix B: Graviton two-point function

For the computation of the geometrical flows we need the second covariant derivative of the diffeomorphism-invariant effective action in combination with the second derivative of the gauge fixing term,  $\nabla_\gamma^2 \hat{\Gamma}_{\text{EH}} + S_{\text{gf}}^{(2)}$ , see (47). For this purpose we need the correction to the second derivative related to the Riemannian connection  $\Gamma_\gamma$ , see e.g. [37]. It is given by

$$\begin{aligned} & \int d^d x'' \left( \Gamma_{\gamma \lambda'' \tau''}^{\mu\nu \rho' \sigma'}(x, x', x'') \frac{\hat{\Gamma}_{\text{EH}}[\bar{g}]}{\delta \bar{g}_{\lambda'' \tau''}(x'')} \right) \\ &= 2\kappa^2 Z_{N,k} \delta(x - x') \sqrt{\bar{g}(x)} \sqrt{\bar{g}(x')} \times \left[ \left( \bar{g}^{\mu\rho'} \bar{g}^{\sigma'\nu} + \bar{g}^{\mu\sigma'} \bar{g}^{\rho'\nu} - \bar{g}^{\mu\nu} \bar{g}^{\rho'\sigma'} \right) \left( \frac{2+d+2\theta d}{8(2+\theta d)} \bar{R} - \frac{4+d+2\theta d}{4(2+\theta d)} \Lambda_k \right) \right. \\ & \quad \left. + \frac{1}{4} \left( \bar{g}^{\mu\nu} \bar{R}^{\rho'\sigma'} + \bar{g}^{\rho'\sigma'} \bar{R}^{\mu\nu} \right) - \frac{1}{4} \left( \bar{g}^{\nu\rho'} \bar{R}^{\sigma'\mu} + \bar{g}^{\nu\sigma'} \bar{R}^{\rho'\mu} + \bar{g}^{\mu\rho'} \bar{R}^{\sigma'\nu} + \bar{g}^{\mu\sigma'} \bar{R}^{\rho'\nu} \right) \right], \end{aligned} \quad (\text{B1})$$

computed at vanishing ghost fields. With (B1) we arrive at

$$\begin{aligned} & \int d^d x d^d x' h(x) \cdot \left( \nabla_\gamma^2 \hat{\Gamma}_{\text{EH}}[\bar{g}] + \mathbf{S}_{\text{gf}}^{(2)}[\bar{g}] \right) (x, x') \cdot h(x') = 2\kappa^2 Z_{N,k} \int d^d x \sqrt{\bar{g}} h_{\mu\nu} \left[ - \left( \frac{1}{2} \delta_{\rho'}^\mu \delta_{\sigma'}^\nu + \frac{\theta^2 - 2\alpha}{4\alpha} \bar{g}^{\mu\nu} \bar{g}_{\rho'\sigma'} \right) \bar{\Delta} \right. \\ & \quad \left. + \frac{2-d}{8(2+\theta d)} \left( 2\delta_{\rho'}^\mu \delta_{\sigma'}^\nu - \bar{g}^{\mu\nu} \bar{g}_{\rho'\sigma'} \right) \bar{R} - \left( \frac{1}{2} - \frac{4+d+2\theta d}{4(2+\theta d)} \right) \left( 2\delta_{\rho'}^\mu \delta_{\sigma'}^\nu - \bar{g}^{\mu\nu} \bar{g}_{\rho'\sigma'} \right) \Lambda_k \right. \\ & \quad \left. + \frac{1}{2} \bar{g}^{\mu\nu} \bar{R}_{\rho'\sigma'} - \bar{R}_{\rho'\sigma'}^{\nu\mu} - \frac{\theta + \alpha}{\alpha} \left( \bar{g}^{\mu\nu} \bar{\nabla}_{\rho'} \bar{\nabla}_{\sigma'} \right) + \frac{1-\alpha}{\alpha} \left( -\delta_{\sigma'}^\mu \bar{\nabla}^\nu \bar{\nabla}_{\rho'} \right) \right] h^{\rho'\sigma'}, \end{aligned} \quad (\text{B2})$$

where  $\bar{\Delta} = \Delta_{\bar{g}}$ . Inserting the York decomposition detailed in Appendix A in (B3) finally leads to

$$\begin{aligned}
\int d^d x d^d x' h(x) \cdot \left( \nabla_{\gamma}^2 \hat{\Gamma}_{\text{EH}}[\bar{g}] + \mathbf{S}_{\text{gf}}^{(2)}[\bar{g}] \right) (x, x') \cdot h(x') &= \kappa^2 Z_{N,k} \int d^d x \sqrt{\bar{g}} \\
&\times \left[ h_{\mu\nu}^T \left[ -\bar{\Delta} + A_T(d, \theta) \bar{R} + H_T(d, \theta) \Lambda_k \right] h^{T, \mu\nu} \right. \\
&+ \frac{2}{\alpha} \hat{\xi}_{\mu} \left[ \left( -\bar{\Delta} - \frac{\bar{R}}{d} \right) \left( -\bar{\Delta} + A_V(d, \alpha, \theta) \bar{R} + H_V(d, \alpha, \theta) \Lambda_k \right) \right] \hat{\xi}^{\mu} \\
&+ C_{S_2}(d, \alpha) \hat{\sigma} \left[ \left( -\bar{\Delta} + A_{S_2}(d, \alpha, \theta) \bar{R} + B_{S_2}(d, \alpha, \theta) \Lambda_k \right) \bar{\Delta} \left( \bar{\Delta} + \frac{\bar{R}}{d-1} \right) \right] \hat{\sigma} \\
&+ 2C_{S_2}(d, \alpha) C_{S_3}(d, \alpha, \theta) \varphi \left[ \bar{\Delta} \left( \bar{\Delta} + \frac{\bar{R}}{d-1} \right) \right] \hat{\sigma} \\
&\left. + C_{S_2}(d, \alpha) C_{S_1}(d, \alpha, \theta) \varphi \left[ -\bar{\Delta} + A_{S_1}(d, \alpha, \theta) \bar{R} + B_{S_1}(d, \alpha, \theta) \Lambda_k \right] \varphi \right], \tag{B3}
\end{aligned}$$

where each line in (B4) contains the kinetic operator of the respective field modes. Note in this context that  $\varphi = \varphi_0 + \varphi_1$  with  $\varphi_0$  being orthogonal to  $\varphi_1$  and  $\hat{\sigma}$ .

The coefficients of the transversal  $h^T$ -mode are

$$\begin{aligned}
A_T(d, \alpha) &= \frac{d(d-1)(2-d) + 4(2+\theta d)}{2d(d-1)(2+\theta d)}, \\
H_T(d, \theta) &= \frac{d}{2+\theta d}, \tag{B4}
\end{aligned}$$

that of the longitudinal mode  $\hat{\xi}$  are

$$A_V(d, \alpha, \theta) = \frac{\alpha d(2-d) - 2(2+\theta d)}{2d(2+\theta d)},$$

$$H_V(\alpha) = -2\alpha.$$

The scalar  $\hat{\sigma}$ ,  $\varphi$ -modes have the curvature-coefficients

$$\begin{aligned}
A_{S_1}(d, \alpha, \theta) &= \\
&= \frac{\alpha(d-2)(d^2 - 2d + 8 + 4\theta d)}{2(2+\theta d)[2\alpha(d-1)(d-2) - (\theta^2 d^2 - 4d - 4\theta)]}
\end{aligned}$$

$$A_{S_2}(d, \alpha, \theta) = \frac{\alpha d(2-d) - 4(2+\theta d)}{2(2+\theta d)[2(d-1) - \alpha(d-2)]},$$

and the coefficients of the cosmological constant terms

$$\begin{aligned}
B_{S_1}(d, \alpha, \theta) &= \\
&= \frac{\alpha d^2(2-d)}{(2+\theta d)[2\alpha(d-1)(d-2) - (\theta^2 d^2 - 4d - 4\theta)]},
\end{aligned}$$

$$B_{S_2}(d, \alpha, \theta) = \frac{\alpha d^2}{(2+\theta d)[2(d-1) - \alpha(d-2)]}.$$

The scalar terms also have the overall prefactors

$$\begin{aligned}
C_{S_1}(d, \alpha, \theta) &= \frac{2\alpha(d-1)(2-d) + (\theta^2 d^2 - 4d - 4\theta)}{2(d-1)[2(d-1) - \alpha(d-2)]}, \\
C_{S_2}(d, \alpha) &= \frac{d-1}{d^2} \frac{2(d-1) - \alpha(d-2)}{\alpha}, \\
C_{S_3}(d, \alpha, \theta) &= \frac{d(-\theta - \alpha) - 2(1-\alpha)}{2(d-1) - \alpha(d-2)}. \tag{B5}
\end{aligned}$$

Particularly interesting for the regulators are the coefficients and prefactor of the kinetic operator  $\Delta_{\bar{g}}$ , see Appendix D.

### Appendix C: Ghost two-point function

As for the graviton we split the ghost into its transverse and longitudinal components and put  $g = \bar{g}$ . In a slight abuse of notation we write

$$C^{\mu} = C^{T, \mu} + \bar{\nabla}^{\mu} \frac{1}{\sqrt{-\bar{\Delta}}} \eta, \quad \bar{C}_{\mu} = \bar{C}_{\mu}^T + \bar{\nabla}_{\mu} \frac{1}{\sqrt{-\bar{\Delta}}} \bar{\eta}, \tag{C1}$$

neglecting the subtleties concerning the inversion of  $\bar{\Delta}$ . In (C1)  $\bar{C}_{\mu}^T$  and  $C^{T, \mu}$  are the transverse components of  $\bar{C}_{\mu}$  and  $C^{\mu}$ , i.e.  $\bar{\nabla}^{\mu} \bar{C}_{\mu}^T = 0$  and  $\bar{\nabla}_{\mu} C^{T, \mu} = 0$ , and  $\eta, \bar{\eta}$  are scalar Grassmann fields. Inserting the parameterisation (C1) in the ghost action, (20), we finally arrive at

$$\begin{aligned}
S_{gh} &= 2 \int d^d x \sqrt{\bar{g}} \bar{C}_{\mu}^T \left( -\bar{\Delta} - \frac{\bar{R}}{d} \right) C^{T, \mu} \\
&+ 2 \int d^d x \sqrt{\bar{g}} \bar{\eta} \left( -\bar{\Delta} - \frac{2\bar{R}}{d} \right) \eta. \tag{C2}
\end{aligned}$$

### Appendix D: Regulators

The following appendix contains the full set of regulators for the flow within the background field approximation, see Section VI. Our choice is adapted to the York transverse-traceless decomposition of the kinetic term as detailed in the last Appendix B. The full regulator is chosen diagonal in the basis in field space provided by the York decomposition. Below we provide the scalar parts of the regulators, the lower indices refer to the modes in field space. With

$$\bar{x} = -\frac{\Delta_{\bar{g}}}{k^2}, \quad (\text{D1})$$

the regulator for a general mode of the York decomposition simply amounts to

$$-\bar{\Delta} \rightarrow -\bar{\Delta} + k^2 r(\bar{x}), \quad (\text{D2})$$

for the terms proportional to  $\bar{\Delta}$  in (B4). This choice respects the diagonality of the York decomposition. For example, the kinetic operator on the  $h^T$ -subspace reads  $-Z_{N,k}\kappa^2\bar{\Delta}$  and hence we choose the regulator

$$(R_k[\bar{g}])_{h^T h^T} = Z_{N,k}\kappa^2 k^2 r(\bar{x}), \quad (\text{D3})$$

where we have dropped the projection operator on the  $h^T$ -subspace. The regulators on the  $h^{TL}$  subspace are given by

$$(R_k[\bar{g}])_{\varphi_1\sigma} = Z_{N,k} C_{S2}(d, \alpha) C_{S3}(d, \alpha) \kappa^2 k^2 \left( -\sqrt{\bar{x} \left( \bar{x} - \frac{\bar{R}/k^2}{d-1} \right)} + \sqrt{\bar{x} - \frac{\bar{R}/k^2}{d-1} + r(\bar{x})} \sqrt{\bar{x} + r(\bar{x})} \right),$$

with  $(R_k)_{\varphi_1\sigma} = (R_k[\bar{g}])_{\sigma\varphi_1}^\dagger$ , as well as

$$(R_k[\bar{g}])_{\sigma\sigma} = Z_{N,k} C_{S2}(d, \alpha) \kappa^2 k^2 r(\bar{x}),$$

and for  $i = 0, 1$ ,

$$(R_k[\bar{g}])_{\varphi_i\varphi_i} = Z_{N,k} C_{S2}(d, \alpha) C_{S1}(d, \alpha) \kappa^2 k^2 r(\bar{x}).$$

The regulator on the  $h_{\mu\nu}^T \times h_{\mu\nu}^T$ -subspace is given by

$$(R_k[\bar{g}])_{\xi\xi} = Z_{N,k} \frac{2}{\alpha} \kappa^2 k^2 r(\bar{x}), \quad (\text{D4})$$

where again we dropped the projection operator. Finally, the regulators of the ghost modes are given by

$$(R_k[\bar{g}])_{\bar{C}^T C^T} = 2k^2 r(\bar{x})$$

$$(R_k^{gh}[\bar{g}])_{\bar{\eta}\eta} = 2k^2 r(\bar{x}), \quad (\text{D5})$$

where we have  $(R_k)_{\bar{C}^T C^T} = -(R_k)_{C^T \bar{C}^T}$  and  $(R_k)_{\bar{\eta}\eta} = -(R_k)_{\eta\bar{\eta}}$ .

### Appendix E: Threshold functions and coefficient functions $\bar{F}_\lambda$ and $\bar{F}_g$

The loop integrals in the flow equations for the couplings are represented by the coefficient functions  $I$ , which are, up to prefactors, the standard threshold functions. In the present case these threshold functions only depend on the constant part  $c_\lambda \lambda$  of the two-point functions. For general regulators (29) with shape function  $r$  the threshold functions read

$$\Phi_n^p(\omega) = \frac{1}{\Gamma(n)} \int_0^\infty dx x^{n-1} \frac{r(x) - xr'(x)}{(x+r(x) + \frac{d}{d-2}\omega)^p},$$

$$\tilde{\Phi}_n^p(\omega) = \frac{1}{\Gamma(n)} \int_0^\infty dx x^{n-1} \frac{r(x)}{(x+r(x) + \frac{d}{d-2}\omega)^p}, \quad (\text{E1})$$

where  $\omega$  is 0 or  $-\lambda$ , depending on the mode considered. The threshold function  $\Phi_n^p$  appears in terms proportional to  $\partial_t r(x)$  leading to the coefficient functions  $I^{(1)}$  in the flow equations. The threshold function  $\tilde{\Phi}_n^p$  appears in terms proportional to  $\partial_t Z$  or  $\partial_t \lambda$ , leading to the coefficient functions  $I^{(2)}$ .

For the flow of the cosmological constants  $\bar{\lambda}$  and  $\lambda$ , (88) and (95) respectively, the coefficient functions read

$$\bar{F}_\lambda^{(1)} = \frac{4\pi g_N}{(4\pi)^{d/2}} \left[ d(d-1) \Phi_{\frac{d}{2}}^1(-\lambda) - d \Phi_{\frac{d}{2}}^1(0) \right],$$

$$\bar{F}_\lambda^{(2)} = \frac{1}{2} \frac{4\pi g_N}{(4\pi)^{d/2}} d(d-1) \tilde{\Phi}_{\frac{d}{2}}^1(-\lambda). \quad (\text{E2})$$

The last coefficient function is that of the ghost loop,  $I_{\lambda, \text{gh}}^{(1)} = I_{\lambda, \text{gh}}$ , there is no term proportional to the wave function renormalisation of the ghost which we dropped in the present analysis.

The coefficient functions in the flow of the Newton constant  $\partial_t \bar{g}_N$  and  $\partial_t g_N$ , (87) and (94) respectively, read

$$\bar{F}_g^{(1)} = 4 \frac{4\pi g_N}{(4\pi)^{d/2}} \left[ a_1 \Phi_{\frac{d-2}{2}}^1(-\lambda) + a_2 \Phi_{\frac{d}{2}}^2(-\lambda) \right]$$

$$- 4 \frac{4\pi g_N}{(4\pi)^{d/2}} \left[ a_3 \Phi_{\frac{d-2}{2}}^1(0) + a_4 \Phi_{\frac{d}{2}}^2(0) \right],$$

$$\bar{F}_g^{(2)} = 2 \frac{4\pi g_N}{(4\pi)^{d/2}} \left[ a_1 \tilde{\Phi}_{\frac{d-2}{2}}^1(-\lambda) + a_2 \tilde{\Phi}_{\frac{d}{2}}^2(-\lambda) \right], \quad (\text{E3})$$

with the parameters  $a_i$ ,

$$a_1 = \frac{d^3 - 2d^2 - 11d - 12}{12(d-1)},$$

$$a_2 = -\frac{d^3 - 2d^2 + 5d - 12}{4(d-1)}, \quad (\text{E4})$$

and

$$a_3 = \frac{d^2 - 6}{6d}, \quad a_4 = \frac{d+1}{d}, \quad (\text{E5})$$

Note that parts of  $\bar{F}_g$  in (E3) stemming from modes without and with explicit curvature-dependence are those proportional to  $\Phi_{\frac{d-2}{2}}^1, \tilde{\Phi}_{\frac{d-2}{2}}^1$ , and  $\Phi_{\frac{d}{2}}^2, \tilde{\Phi}_{\frac{d}{2}}^2$ , respectively. Hence, it is the index  $p-1 = 0, 1$  of  $\Phi^p, \tilde{\Phi}^p$  which labels the modes without,  $p-1 = 0$ , and with,  $p-1 = 1$ , curvature-dependence.

### Appendix F: Threshold functions and coefficient functions $F_\lambda$ and $F_g$ for the optimised regulator

For the optimised regulator the threshold functions (E1) in Appendix A read,

$$\Phi_n^p(\omega) = \frac{1}{n\Gamma(n)} \frac{1}{(1 + \frac{d}{d-2}\omega)^p}, \quad (\text{F1})$$

$$\tilde{\Phi}_n^p(\omega) = \frac{1}{n+1} \Phi_n^p(\omega). \quad (\text{F2})$$

Eq. (F1) implies that

$$\tilde{\Phi}_{\frac{d-2}{2}}^p(\omega) = \frac{2}{d} \Phi_{\frac{d-2}{2}}^p(\omega), \quad \tilde{\Phi}_{\frac{d}{2}}^p(\omega) = \frac{2}{d+2} \Phi_{\frac{d}{2}}^p(\omega). \quad (\text{F3})$$

Inserting these relations into (E2), (E3), leads to (93) with the subscript  $p-1 = 0, 1$  labels the curvature-dependence. Then the  $\bar{F}_\lambda$ 's, (E2), used in Section VII for the flow of the background dynamical cosmological constant, are given by

$$\begin{aligned} \bar{F}_\lambda^{(1)} &= 6 \frac{g_N}{4\pi} \left( -\frac{2}{3} + \frac{1}{1-2\lambda} \right), \\ \bar{F}_\lambda^{(2)} &= \frac{g_N}{4\pi} \frac{1}{1-2\lambda}. \end{aligned} \quad (\text{F4})$$

Eq. (F5) leads to the coefficients  $I_\lambda$ ,

$$\begin{aligned} I_{\lambda,-2} &= \frac{g_N}{4\pi} \frac{1}{1-2\lambda} \\ I_{\lambda,\text{gh}} &= -\frac{g_N}{4\pi} \frac{4}{3}, \end{aligned} \quad (\text{F5})$$

with  $I_{\lambda,\text{gh}} = -2I_{\lambda,0}$ . The  $\bar{F}_g$ 's, (E3), used in Section VII for the flow of the background cosmological constant, (90), are given by

$$\begin{aligned} \bar{F}_g^{(1)} &= -4 \frac{g_N^2}{4\pi} \left( \frac{25}{24} + \frac{2}{3} \frac{1}{1-2\lambda} + \frac{5}{3} \frac{1}{(1-2\lambda)^2} \right), \\ \bar{F}_g^{(2)} &= -\frac{g_N^2}{6\pi} \left( \frac{1}{1-2\lambda} + \frac{5}{3} \frac{1}{(1-2\lambda)^2} \right). \end{aligned} \quad (\text{F6})$$

Eq. (F7) leads to the coefficients  $I_N$ ,

$$\begin{aligned} I_{N,-2} &= -\frac{g_N^2}{6\pi} \left( \frac{1}{1-2\lambda} + \frac{5}{3} \frac{1}{(1-2\lambda)^2} \right), \\ I_{N,\text{gh}} &= -\frac{4}{3} \frac{g_N}{3\pi} \frac{25}{24}, \\ I_{N,\text{gh},1} &= -\frac{1}{3} \frac{g_N}{3\pi} \frac{25}{24}, \end{aligned} \quad (\text{F7})$$

with  $I_{N,\text{gh}} = -2I_{N,0}$ . For the ghost coefficients we have used that the term independent of  $\lambda$  in first line of (F6) stems from the sum of ghost  $I_{N,\text{gh}} + I_{N,0} = 1/2I_{N,\text{gh}}$ . We get with (89) and (F3) with  $d = 4$  that

$$-4 \frac{g_N^2}{4\pi} \frac{25}{24} = 2I_{N,\text{gh},0} + 3I_{N,\text{gh},1}, \quad I_{N,\text{gh},1} = \frac{1}{3} I_{N,\text{gh},0}. \quad (\text{F8})$$

This leads to the  $I_{\text{ghost}}$  in (F7). The coefficients  $I_{N,-2,0}$  and  $I_{N,-2,1}$  are given by the terms in the first line of (F7) which are proportional to  $(1-2\lambda)^{-1}$  and  $(1-2\lambda)^{-2}$  respectively.

For the computation of the flow of the dynamical couplings we simply have to insert the coefficients  $I_\lambda$  and  $I_N$  in (F5),(F7),(84) in (94),(95). This leads us to the following expressions for the right hand sides  $F_g, F_\lambda$  of the dynamical flows (51),

$$\begin{aligned} F_g(g_N, \lambda) &= -\frac{g_N^2}{3\pi} \left( \frac{5}{3} \frac{25}{24} + \frac{1}{1-2\lambda} + \frac{5}{3} \frac{1}{(1-2\lambda)^2} \right) \\ &+ \left( \eta_N + \dot{\lambda} \partial_\lambda \right) \frac{g_N^2}{6\pi} \left( \frac{1}{1-2\lambda} + \frac{5}{3} \frac{1}{(1-2\lambda)^2} \right), \end{aligned} \quad (\text{F9})$$

and

$$\begin{aligned} F_\lambda(g_N, \lambda) &= -\frac{g_N}{2\pi} \left( \frac{2}{3} - \frac{1}{1-2\lambda} \right) \\ &- \left( \eta_N + \frac{2\partial_t \lambda}{1-2\lambda} \right) \frac{g_N}{4\pi} \frac{1}{1-2\lambda}. \end{aligned} \quad (\text{F10})$$

- 
- [1] S. Weinberg, General Relativity: An Einstein centenary survey, Eds. Hawking, S.W., Israel, W; Cambridge University Press , 790 (1979).
- [2] C. P. Burgess, Living Rev. Rel. **7**, 5 (2004), gr-qc/0311082.
- [3] M. Niedermaier and M. Reuter, Living Rev.Rel. **9**, 5 (2006).
- [4] H. W. Hamber, Gen.Rel.Grav. **41**, 817 (2009), 0901.0964.
- [5] J. Ambjorn, J. Jurkiewicz, and R. Loll, Lect.Notes Phys. **807**, 59 (2010), 0906.3947.
- [6] M. Reuter and F. Saueressig, (2007), 0708.1317.
- [7] R. Percacci, (2007), 0709.3851.
- [8] D. F. Litim, Phil.Trans.Roy.Soc.Lond. **A369**, 2759 (2011), 1102.4624.
- [9] J. M. Pawłowski, Annals Phys. **322**, 2831 (2007), hep-th/0512261.
- [10] H. Gies, (2006), hep-ph/0611146.
- [11] O. J. Rosten, (2010), 1003.1366.
- [12] M. Reuter and F. Saueressig, (2012), 1202.2274.
- [13] M. Reuter, Phys. Rev. **D57**, 971 (1998), hep-th/9605030.
- [14] S. Falkenberg and S. D. Odintsov, Int.J.Mod.Phys. **A13**, 607 (1998), hep-th/9612019.
- [15] W. Souma, Prog.Theor.Phys. **102**, 181 (1999), hep-th/9907027.
- [16] A. Codello, R. Percacci, and C. Rahmede, Int. J. Mod. Phys. **A23**, 143 (2008), 0705.1769.
- [17] P. F. Machado and F. Saueressig, Phys. Rev. **D77**, 124045 (2008), 0712.0445.
- [18] A. Codello and R. Percacci, Phys. Rev. Lett. **97**, 221301 (2006), hep-th/0607128.
- [19] F. Saueressig, K. Groh, S. Rechenberger, and O. Zanusso, (2011), 1111.1743.
- [20] K. Groh and F. Saueressig, J. Phys. **A43**, 365403 (2010), 1001.5032.
- [21] A. Eichhorn, H. Gies, and M. M. Scherer, Phys. Rev. **D80**, 104003 (2009), 0907.1828.
- [22] A. Eichhorn and H. Gies, Phys. Rev. **D81**, 104010 (2010), 1001.5033.
- [23] E. Manrique, S. Rechenberger, and F. Saueressig, Phys.Rev.Lett. **106**, 251302 (2011), 1102.5012.
- [24] R. Percacci and D. Perini, Phys. Rev. **D67**, 081503 (2003), hep-th/0207033.
- [25] J.-E. Daum, U. Harst, and M. Reuter, JHEP **1001**, 084 (2010), 0910.4938.
- [26] U. Harst and M. Reuter, JHEP **05**, 119 (2011), 1101.6007.
- [27] A. Eichhorn and H. Gies, (2011), 1104.5366.
- [28] S. Folkerts, D. F. Litim, and J. M. Pawłowski, (2011), 1101.5552.
- [29] M. Reuter and H. Weyer, Phys. Rev. **D79**, 105005 (2009), 0801.3287.
- [30] N. Nielsen, Nucl.Phys. **B101**, 173 (1975).
- [31] V. Branchina, K. A. Meissner, and G. Veneziano, Phys.Lett. **B574**, 319 (2003), hep-th/0309234.
- [32] J. M. Pawłowski, (2003), hep-th/0310018.
- [33] I. Donkin, Diploma thesis, Heidelberg (2008).
- [34] E. Fradkin and A. A. Tseytlin, Nucl.Phys. **B234**, 509 (1984).
- [35] G. Vilkovisky, Nucl.Phys. **B234**, 125 (1984).
- [36] B. S. DeWitt, Quantum Field Theory and Quantum Statistics, Vol. 1, Batalin, I.A. (Ed.) et al. , 191 (1988).
- [37] B. S. DeWitt, Int.Ser.Monogr.Phys. **114**, 1 (2003).
- [38] C. Burgess and G. Kunstatter, Mod.Phys.Lett. **A2**, 875 (1987).
- [39] G. Kunstatter, Class.Quant.Grav. **9**, S157 (1992).
- [40] E. Manrique, M. Reuter, and F. Saueressig, Annals Phys. **326**, 463 (2011), 1006.0099.
- [41] J. M. Pawłowski, Int.J.Mod.Phys. **A16**, 2105 (2001).
- [42] D. F. Litim and J. M. Pawłowski, Phys. Rev. **D66**, 025030 (2002), hep-th/0202188.
- [43] D. F. Litim and J. M. Pawłowski, JHEP **0209**, 049 (2002), hep-th/0203005.
- [44] D. F. Litim and J. M. Pawłowski, Phys. Lett. **B546**, 279 (2002), hep-th/0208216.
- [45] J. Braun, H. Gies, and J. M. Pawłowski, Phys. Lett. **B684**, 262 (2010), 0708.2413.
- [46] D. F. Litim, Phys. Lett. **B486**, 92 (2000), hep-th/0005245.
- [47] O. Lauscher and M. Reuter, Phys. Rev. **D65**, 025013 (2002), hep-th/0108040.
- [48] D. F. Litim, Phys. Rev. Lett. **92**, 201301 (2004), hep-th/0312114.
- [49] D. Benedetti, K. Groh, P. F. Machado, and F. Saueressig, JHEP **1106**, 079 (2011), 1012.3081.
- [50] J.-P. Blaizot, J. M. Pawłowski, and U. Reinosa, Phys.Lett. **B696**, 523 (2011), 1009.6048.
- [51] C. Contreras and D. F. Litim, in preparation.
- [52] H. Gies, Phys.Rev. **D66**, 025006 (2002), hep-th/0202207.
- [53] E. Manrique, M. Reuter, and F. Saueressig, Annals Phys. **326**, 440 (2011), 1003.5129.